UNIVERSIDAD NACIONAL AUTÓNOMA DE MÉXICO

PROGRAMA DE MAESTRIA Y DOCTORADO EN INGENIERIA

MECÁNICA - TERMOFLUIDOS

Colapsos de Columnas Granulares

TESIS

QUE PARA OPTAR POR EL GRADO DE:

DOCTOR EN INGENIERIA

PRESENTA:

Horacio Tapia McClung

TUTOR: Roberto Zenit Camacho

Instituto de Investigaciones en Materiales,

Universidad Nacional Autónoma de México

MÉXICO, D.F. NOVIEMBRE 2012

JURADO ASIGNADO:

Presidente: Dr. Solorio Ordaz Francisco Javier

Secretario: Dra. Garza Hume Clara Eugenia

Vocal: Dr. Zenit Camacho José Roberto
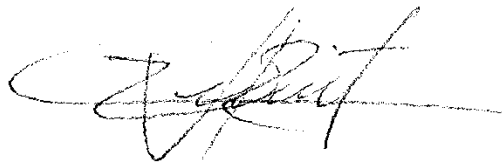
1$^{er.}$ Suplente: Dr. Caballero Robles Gabriel

2$^{do.}$ Suplente: Dr. Boyer Denis Pierre

Lugar o lugares donde se realizó la tesis:

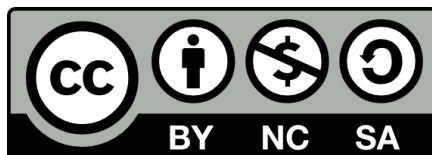Instituto de Investigaciones en Materiales, Universidad Nacional Autónoma de México

TUTOR DE TESIS:
Dr. Roberto Zenit Camacho

_____

FIRMA

Con todo mi amor,
a
Martha
y
Julia.

RESUMEN

COLAPSOS DE COLUMNAS GRANULARES

Horacio Tapia McClung

Instituto de Investigaciones en Materiales,

Universidad Nacional Autónoma de México

En este trabajo se presenta un análisis dimensional y de escalamiento del colapso de columnas granulares, explorando los parámetros asociados por medio de simulaciones numéricas. Por medio del *Teorema Pi-Buckingham* y de la auto-similaridad, construimos las leyes de escalamiento observadas experimentalmente para las alturas máximas de las columnas, que dependen de la relación entre la altura y el ancho inicial de la columna por medio de una ley de potencias. Se discuten los parámetros adimensionales obtenidos y se exploran los efectos que éstos tienen en relación con el flujo granular generado durante el colapso de columnas bidimensionales por medio de simulaciones numéricas basadas en el método del elemento discreto. Por un lado, se presentan resultados sobre el efecto de formar las columnas con granos alargados, estudiando los colapsos variando el parámetro de relación de aspecto inicial y el alargamiento de los granos, encontrando que las distancias finales que caracterizan los depósitos siguen las mismas leyes de potencia independientemente del tipo de grano utilizado para formar la columna. Por otro lado estudiamos los colapsos de columnas formadas por granos circulares que ocurren en diferentes gravedades, dadas por múltiplos del valor nominal de la gravedad en la Tierra. Se encuentra que cuando las mediciones se escalan de manera apropiada, las distancias finales, particularmente la altura máxima de los depósitos, ocurren de manera similar independiente del valor de la gravedad en

donde ocurren o del valor de la fricción entre los granos que forman las columnas, y en todos los casos las alturas finales de los depósitos siguen las mismas leyes de escalamiento reportadas. La invariancia de las leyes de escalamiento son indicativas de la auto-similaridad de las propiedades finales del colapso de columnas granulares y justifican el uso del análisis dimensional para obtener dichas leyes de escalamiento.

ABSTRACT

COLLAPSES OF GRANULAR COLUMNS

Horacio Tapia McClung

Instituto de Investigaciones en Materiales,

Universidad Nacional Autónoma de México

This work presents a dimensional analysis of the collapse of granular columns and explores the effect of the dimensionless parameters using numerical simulations. By means of the *Buckingham-Pi Theorem* and self-similarity, we obtain the power law scaling observed experimentally for the maximum height of the columns, depending only on the ratio between the initial height and width of the columns. The dimensionless parameters obtained are discussed and their effects on the granular flow are explored for the collapse using numerical simulations based on the discrete element method. Results of collapses of columns made of elongated grains are presented, in which the initial aspect ratio parameter is varied together with the elongation of the grain, finding that the scaling laws are preserved and depend weakly on the type of grain used. On the other hand, the effect of gravity is studied by collapsing columns under different gravitational accelerations, given as multiples of the value on Earth, for columns made of grains with different friction values. In this case it is found that, when scaled appropriately, the maximum height of the columns does not depend on the value of gravity and the final height still scales with the initial aspect ratio as a power law. The invariance of the scaling laws to the dimensionless parameters explored are indicative of the self-similarity of the final distances of the collapse, and justify the way the scaling laws are obtained by making use of dimensional analysis.

AGRADECIMIENTOS

A todos los que se han visto involucrados de alguna u otra forma en este proceso, gracias por su apoyo y su ayuda. Sin ustedes no hubiera sido posible concluir esta tesis: Martha gracias por tu amor todos estos años; Julia quien ha dado una alegría diferente a mi vida en estos meses. A mi madre Emily, mi padre Horacio y mi hermano Rodrigo, porque todo lo que soy se lo debo a ellos.

A todos los amigos, los nuevos y los antiguos, con los que que al paso de los años seguimos en la lucha: Martha, Nettel, Ro, Mario, Javier, Sergio, Stella, Rodrigo, Alicia, Cruz, Oscar, Joel, Eric, Carmen, Carla, Camila, Guille, Tacho, Estaiby; a todos con lo que me he cruzado en el camino y espero seguirlo haciendo. A los colegas y amigos del laboratorio de reología, empezando por el comandante, Roberto, Ernesto, Oscar, Paco, Caro, Esli, Roger, Charly, René, Enrique(s), Cris; por las horas de terror urbano durante las que podia analizar datos y por el café.

Al Doctor Roberto Zenit Camacho, amante de los fluidos y burbujas, tutor, profesor, guía, colaborador y amigo, quien abrió las puertas de su laboratorio para poder desarrollar este trabajo, y quien contagia de una forma especial el gusto que tiene por los flujos burbujantes a todos a su alrededor. Gracias Roberto por la ayuda, el apoyo y sobre todo las ideas.

A todos los miembros del comité tutoral y del jurado que han revisado este trabajo; profesores de excelente calidad humana y académica, les agraezco haberse

tomado el tiempo y el esfuerzo de leer y revisar cada una de las partes de este documento. Gracias por sus críticas y sus observaciones sobre este trabajo, las cuales han contribuido a mejorarlo y han dado lugar a nuevas ideas, contribuyendo asi al desarrollo del conocimiento en ésta área.

Al programa del Posgrado de Ingeniería de la Universidad Nacional Autónoma de México, administrativos, docentes y académicos, gracias por su esfuerzo y dedicación en beneficio de nuestro México.

Finalmente, un agradecimiento al Departamento de Física de la Universidad Veracruzana en donde se realizaron algunas simulaciones y al Laboratorio Nacional de Informática Avanzada LANIA, por proporcionar un espacio en el cual ha sido posible finalizar este proyecto.

Xalapa, Ver.

Noviembre de 2012.

CONTENTS

CHAPTER 1

INTRODUCTION

Granular media are ubiquitous and fundamental to a large number of natural phenomena and anthropogenic processes. Many of these involve static piles, Fig. 1.1a, that result from the accumulation of material and/or the collective flow of particles on spatial scales ranging from millimeters to several kilometers, Fig. 1.1b. These two features of granular media, the tendency to remain static and the flow properties they display, are important in natural processes such as erosion or sedimentation, and in catastrophic events such as landslides or volcanic eruptions [30].

Despite being so common, the behavior of these systems consisting primarily of large collections of individual particles of different shapes and sizes, is far from simple and is not yet well understood. From the problem of the distribution of pressure in a static pile of granular material, to the observed complex flows that can develop under external forces, there is as yet no theory that describes completely the observations, and in many cases prediction is still a challenge [16, 18].

Due to the lack of a theoretical model similar to that of a Newtonian fluid or a Hookean solid, research on granular media has focused on the analysis of simple flows that can be controlled and reproduced in the laboratory, an approach that has provided some understanding of the basic processes involved. An example of this kind of flow that has received much attention in recent years due to its
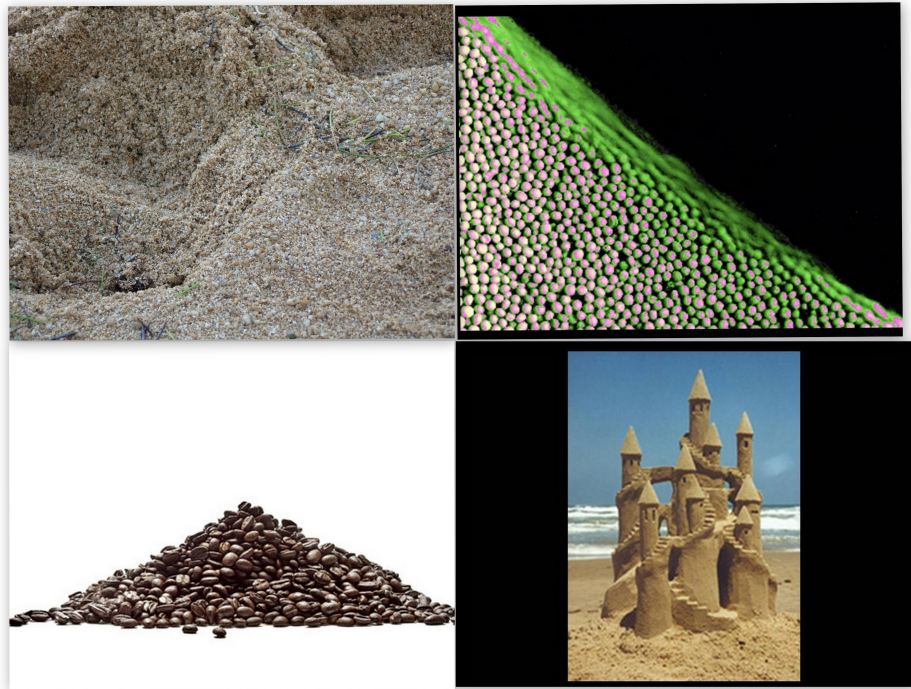
(a) Examples of static piles and flows of granular materials.

(b) Natural processes involving a granular flowing phase.

Figura 1.1: Examples of granular materials.
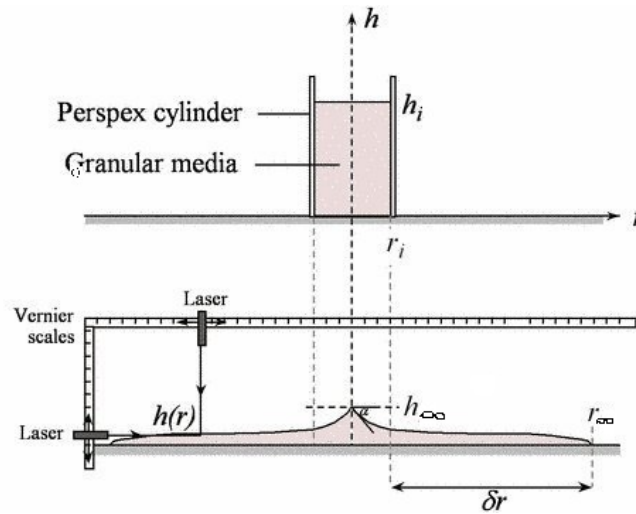
Figura 1.2: Sketch of the granular column collapse experiment. The top figure shows the initial state before the walls are removed, the bottom figure shows the final state after the walls have been removed. Figure from [30]. In the top figure h_i, x_i represent the initial height and radius of the column, while in the bottom figure $\delta r = r_\infty - r0$ is the run out distance while h_∞ represents the final height of the deposit.

simplicity and the rich dynamics observed, is the collapse of a granular column [3, 19, 22, 24, 25, 26, 27, 28, 29, 30, 39, 40, 43, 46].

This simple table-top experiment is partly inspired by the flows of mass in which the granular phase dominates, for example, geophysical events such as avalanches, rock, mud-slides or landslides on a cliff, where the material moves as a granular flow initiated by its own weight (Fig. 1.1b), and serves as a paradigm for the study of processes that can be observed at a larger scale, thus becoming a test case for the development of numerical and theoretical models for granular media (for example [21, 22, 24, 30, 39]), and for studying similar extraterrestrial events [26, 36].

1.1.   The collapse of a granular column

This simple experiment consists of the quick release of a column made of some granular material like sand, rice, seeds or glass beads, over a horizontal surface, and study the process leading to the final emplacement (Fig. 1.2). It has been found that the final state of the deposits, characterized by the total distance traveled by the grains on the horizontal surface, denoted by x_∞ and the fi-

nal height of the deposit after the collapse, depends only on the ratio of initial height and width of the column, $a = h_0/x_0$. Measurements that allow study of the dynamics of the process as the collapses occur also reveal interesting characteristics of the transient flow. Whereas the measured properties seem to depend on the initial aspect ratio of the columns, it appears that this dependence is weak in other variables determining physical characteristics of the material used, for example, the shape, size or frictional properties of the grains. These seem not to contribute greatly in determining the final properties of the emplacements, and neither does the substrate of the surface on which the collapses occur [3, 19, 22, 24, 25, 26, 27, 28, 29, 30, 39, 40, 42, 43, 44, 46].

1.2.   Scaling and similarity

That the final properties of the emplacements scale only with the initial aspect ratio of the columns has been confirmed by several experiments and numerical simulations using different materials and in different configurations. An incomplete list of governing parameters influencing the collapse of a granular column over a horizontal surface could be: the initial conditions, h_0, x_0; physical and mechanical properties of the grains like the mean diameter d and density ρ; the value of the local gravitational acceleration g; externally applied normal and shear stresses P, σ; the friction coefficient between grains μ and other friction properties; the width of channel, etc.

In order to study the process, among all the possible variables that could affect the outcome, only those with most direct influence that seem relevant and can be controlled experimentally are chosen.

A tool for gaining insight into how a dependent variable, for example the final height of the deposit after the grains have come to rest, h_∞ (see bottom of Figure 1.2), depends on the relevant governing variables, such as the initial conditions h_0, x_0, gravity g, density ρ, mean diameter d and external stresses P, σ, is Dimensional Analysis. This tool allows study of a system that depends on many governing parameters in such a way that relevant scaling laws are revealed.

A simple example is the classical frictionless pendulum, which is worked out in detail in Chapter 3, where dimensional analysis is used to show that the period of

oscillation T of a finite mass m hanging from a massless string of length l moving only on a plane with no friction with its surroundings, under the acceleration of gravity g, can be expressed as a dimensionless function that takes the form

$$T = const \times \sqrt{l/g}.$$

For the problem of the final height of the emplacement after the granular column has collapsed, we can write

$$h_\infty = H(\rho, d, P, \sigma, g, h_0, x_0, \mu).$$

Using dimensional analysis it is possible to write, for example,

$$\frac{h_\infty}{h_0} = \Pi\left(\frac{P}{\rho g h_0}, \frac{\sigma}{\rho g h_0}, \frac{x_0}{h_0}, \frac{d}{h_0}, \mu\right).$$

The dependence on the three governing parameters ρ, g, h_0 is "absorbed" into dimensionless quantities that are combinations of the relevant parameters. The function Π is a dimensionless function describing the dependence of the final height in terms of $k = 4$ dimensionless parameters, as opposed to the original $n = 7$ governing parameters.

The initial aspect ratio appears naturally as a dimensionless argument as x_0/h_0. In all the experiments the ratio of typical grain size to the height of the column is small, $d/h_0 \ll 1$. If, by the end of the collapse the ratio of the externally imposed stresses to the weight of the column is negligible, then for the final height of the emplacement we can write

$$\frac{h_\infty}{h_0} = \Pi_1(a),$$

where $a = h_0/x_0$ is the initial aspect ratio of the column, and the function Π_1 is assumed to exist in the desired limits. The formalism developed by Barenblatt [4], that will be presented in a following chapter, permits the assumption that the function Π_1 depends as a power law on the parameter a as

$$\frac{h_\infty}{h_0} \sim a^\beta,$$

which is precisely the scaling law observed experimentally and confirmed by se-

veral works.

Unfortunately, neither dimensional analysis nor the approach developed by Barenblatt [4] gives us any information on the value of the scaling exponent β in the above expression; this has to be obtained by means of experiments or numerical simulations. The observed scaling law, which can be constructed by means of scaling assumptions, reveals a fundamental property of the system: the final properties of the collapse of a granular column are self-similar in the initial aspect ratio of the column.

1.3. Previous experimental and numerical work

Much of the work done on the problem of the collapse of a granular column has been devoted to reproducing the scaling laws observed in the original experiments and to find them under different conditions [3, 26, 29, 43]. Other research has employed numerical simulations to search for these scaling laws while providing details of the collapse process [22, 39, 40, 46].

Some research has been done using a simple model based on a continuum description [3, 27, 33] that reproduces the observations in certain ranges of the relevant parameters. A detailed numerical simulation using a model for granular rheology [21, 23] has shown that the deposit's final properties scale with the initial aspect ratio of the column.

Very few studies have addressed the dependence on other parameters. Until recently, the shape of the grains used to make the columns was studied in a systematic way experimentally [44] and numerically [42], and remarkably, in both cases a similar scaling law was found, suggesting that the shape of the grains used weakly affects the final properties of the collapse.

Analytically, it is a difficult problem to study due to the lack of a well established theory, but dimensional arguments can be used to obtain these scalings from simple models [24]. Recently, a rheology for granular flows has been suggested [13, 17] and used with some success to reproduce the observations of the collapse of granular columns [21, 23] using numerical simulations.

This so called μ-rheology describes the frictional properties of the flow by means of a single dimensionless quantity called the inertial number, I. The numerical simulations performed using this model for the flow friction properties [21, 23] are able to reproduce the observed scaling properties of the system.

1.4.   Original contribution

There is yet no satisfactory explanation of why the final properties of the deposits made from collapses of dry granular columns scale only with the initial aspect ratio of the column. Heuristic models based on the experimental observations [24] or continuum based models and numerical simulations [3, 21, 23, 27, 33] do not provide a general framework to understand these scalings. The fundamental goal of this research is to show that the scaling law

$$\frac{h_\infty}{h_0} = a^\beta,$$

for the final height of the deposits, can be understood using scaling arguments based on well established experimental and numerical results. The details of the assumptions leading to this relationship are the core of this thesis.

The way this work contributes to the problem of the granular column collapse is in that it provides a description of the final properties of the deposits using a systematic analysis of the relevant parameters governing the process. To better understand the effect of relevant parameters on the collapse of granular columns, the value of the local gravitational acceleration, the coefficient of friction between grains and the elongation of the grains forming the column are varied in this study.

The effect of gravity is relevant because the collapse of a column occurs due to its own weight. It is the weight of the column that causes the grains to be in contact, thus the importance of the friction between grains. The elongation of the grains is relevant to understand the differences from the case of circular grains with respect to friction and granular flow.

The results of collapses of granular columns made of elongated grains have been published as an article in a specialized journal [42], and is one of the main contributions of this thesis to the problem of the collapse of a granular column, as it is,

together with [44], one of the first systematic studies of the problem using elongated grains to conform the columns. It is relevant to the problem because not much is known of the collapses of columns made of grains with different shapes.

This thesis is divided as follows: in Chapter 2 we present the main results of the collapse of a granular column with an emphasis on the relevant parameters. Next, on Chapter 3, the self-similarity and scaling theory is presented, followed by Chapter 4, on the numerical method used. In Chapter 5 we use the theory of Chapter 3 to solve a simple model for granular flow in the context of the collapse of a column. The study of the dependence of the elongation of the grains is considered in Chapter 6, followed by the results of varying the value of gravity, Chapter 7. We finish with concluding remarks and suggestions for future work.

CHAPTER 2

THE COLLAPSE OF A GRANULAR COLUMN

One of the simplest configurations in which a granular flow can develop in the absence of other external forces (in addition to the acceleration due to gravity), is the collapse of a granular column. This experiment can be seen as a paradigm of phenomena such as sedimentation, erosion or catastrophic events such as avalanches and landslides.

Despite the simplicity of the experiment, it presents complex and rich dynamics and, like many other phenomena involving granular media, the observed behavior is still not well understood. Early research on this problem focused primarily on the description of the deposit's final state, starting from a cylindrical configuration in which the material used (grain type), the initial height and initial radius of the column and the type of surface on which the collapse occurs was varied. Figure 2.2 shows a schematic of the original experiments.

In this chapter we present the fundamental results of the scaling of the final properties of the deposits found experimentally and numerically on the published literature, emphasizing on the 2 dimensional configuration's results and on the parameters explored (size, shape, dimensions, friction coefficients, etc.). Likewise, notation to be used in the remainder of this work is introduced.

Figura 2.1: Example of materials used for the collapse of granular columns. Figure from [30].

d [cm]	$h_0[cm]$	$\mu = \text{tg}(\delta)$	Other grain properties	Reference
0.035	0.7-25	0.4	glass beads, $\rho = 2500 kg/m^3$	[24]
0.032	1.8-46.5	0.6	sand, $\rho = 2600 kg/m^3$	[30]
0.7×0.2	2.8-64.2	0.6	rice, $\rho = 1460 kg/m^3$	[30]
0.08	4-40	0.7	grit, $\rho = 2600 kg/m^3$	[3]
0.1	4-40	0.45	glass beads, $\rho = 2500 kg/m^3$	[3]
0.015	1.4-14.8	0.56	quartz sand, $\rho = 2600 kg/m^3$	[28]
0.1	1.95-40.95	0.7	sugar, $\rho = 1580 kg/m^3$	[28]
0.7×0.2	1.95-35.1	0.6	rice, $\rho = 1460 kg/m^3$	[28]
0.25	4.8-38	0.43	polypropylene $\rho = 946 kg/m^3$	[22]

Tabla 2.1: Typical properties of grains used in experiments of the collapse of granular columns.

2.1.   Description of the problem

The original experiments [24, 30] consist of a cylindrical container of radius x_0, filled with granular material (for example sand, salt, rice, etc.., Fig. 2.1) up to an initial height h_0.

At the beginning of the experiment, the cylindrical container is quickly removed causing the material to flow axisymmetrically. When the flow comes to rest, the final distance traveled in radial direction, x_∞, and the final height of the deposit, h_∞, are measured, as depicted on Fig. 2.2. In a variant of the original experiment, a rectangular container was used [3, 22, 28, 29]; the process is similar, with a gate rising to allow the material to flow effectively in a single direction (Fig. 2.3).

In both experimental settings, it was found that the quantities characterizing the
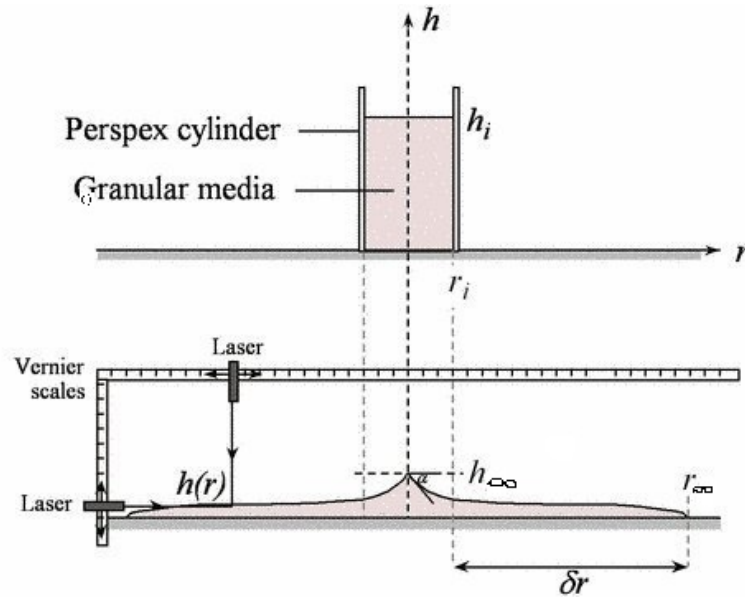
Figura 2.2: Sketch of the granular column collapse experiment. Same as Fig. 1.2. Figure from [30].
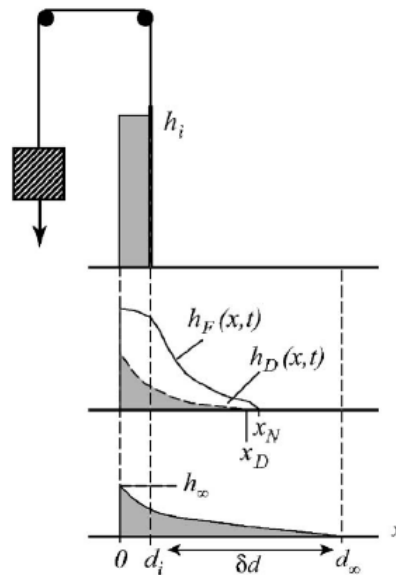

Figura 2.3: Sketch of the granular column collapse experiment in a rectangular container. Figure from [29].

final state of the deposits, namely x_∞ and h_∞, do not depend on the type of granular material used, which implied a weak dependence on the frictional properties of grains. In fact, it was found that these final quantities depend only on the ratio between the initial height and initial radius of the columns, which became known as the initial aspect ratio parameter, $a = h_0/x_0$ with fluctuations inside the limit of experimental error in both axisymmetric and rectangular configurations [3, 22, 28, 29].

The final properties x_∞ and h_∞ scale as a power law $\sim \lambda a^\beta$, where the scaling exponent β varies depending on the range of values of a and seems to depend weakly on grain properties like shape or size, while the scaling coefficient λ shows some dependence on the frictional properties of the grains used and on interactions with boundaries of the container.

The existence of a scaling law that describes the final properties of the emplacements formed by collapses of granular materials that depends weakly on the frictional properties of the system comes as a big surprise. No satisfactory explanation exists yet to account for these observations.

The evolution of the collapse also depends on the initial aspect ratio of the column [11, 24, 30]: for wide columns, $a < 1$, the collapse occurs over a well defined sliding plane and only the grains that are near the edges of the column participate in the flow with a big number of them staying still in the center region of the column.

As the value of a increases, the angle of the sliding plane with respect to the horizontal surface increases and becomes less defined, causing more grains to participate in the collapse and subsequent flow. For intermediate values of a, the collapse occurs on planes that make a well defined conical pile made of grains remaining still during the process, while others flow as an avalanche over the free surface. The shape of the cone is related to the frictional properties of the material used [24] and to the initial preparation of the samples [9].

2.2.   Summary of Experimental Results

The observation that final properties of the emplacements after the column has collapsed depend on the column's initial aspect ratio has been established by several experiments [3, 11, 24, 25, 28, 29, 30]. In the remainder of this work we will

use the notation h_0, x_0 for the initial height and width of the column. In axisymmetric experiments, x_0 corresponds to the radius of the cylindrical column, while in two dimensional experiments it refers to the initial width of the container. The normalized run-out distance and final height of the deposit are usually reported as

$$x^* = \frac{x_\infty - x_0}{x_0} \tag{2.1}$$

$$h^* = \frac{h_\infty}{x_0} \tag{2.2}$$

and used to identify the scaling laws of the form

$$x^*, h^* = \lambda_i a^{\beta_i}. \tag{2.3}$$

The main experimental results are shown in Table 2.2. It is interesting to note the transition from a linear dependence to a power law in the scaling relation as the initial aspect ratio of the column varies from small to larger values, most notable for the normalized run out distance. We focus our attention on the experiments performed on a rectangular container [3, 22, 25, 28], referred to as unidirectional in Table 2.2. It is convenient to express the final height of the column as

$$h^* = \frac{h_\infty}{h_0} \tag{2.4}$$

instead of Eqn. 2.2, i.e., normalized by the initial height of the column h_0. Expressed like this, the data for the normalized height of the deposits are shown in Table 2.3. The experimental results are not conclusive on the value of the scaling exponent, either for the final runout distance or the final height of the deposits.

For the final height of the deposit, values of β obtained experimentally differ slightly from one experiment to another, but are all in the same range regardless of the materials used: looking carefully at the data of Table 2.3, we see that the difference between scaling exponents is no more than 10 percent between the greatest ($\beta = -0.55$) and the lowest ($\beta = -2/3$) values.

Notice from the information on Table 2.3 that the scaling exponent is, in all cases, equal to unity for values of the initial aspect ratio a below a çritical"value, indicating a transition on the scaling as the initial aspect ratio increases. This is consistent

$x^* = (x_\infty - x_0)/x_0$	$h^* = h_\infty/x_0$	Observations	Reference
$\propto a(a < 3)$	$a(a < 0.74)$	Axysimmetric	[24]
$\propto a^{1/2}(a > 3)$	$0.74(a > 0.74)$		
$1.24a(a < 1.7)$	$a(a < 1)$	Axysimmetric	[30]
$1.6a^{1/2}(a > 1.7)$	$0.88a^{1/6}(1.7 < a < 10)$		
$\propto a^{0.55}(w = 1cm, a > 2)$	$\propto a^{0.45}(a > 1.5)$	Unidirectional	[3]
$\propto a^{0.9}(w = 20cm, a > 2)$			
$\propto a(a < 3)$	$\propto a(a < 0.7)$	Unidirectional	[25]
$\propto a^{2/3}(a > 3)$	$\propto a^{1/3}(a > 0.7)$		
$1.6a(a < 1.8)$	$\propto a^{2/5}(a > 1.15)$	Unidirectional	[28]
$2.2a^{2/3}(a > 2.7)$			
$1.2a(a < 1.8, symmetric)$			
$1.9a^{2/3}(a > 2.7, symmetric)$			
$\propto a(a < 2.2)$	$\propto a^{0.45}(d = 2.5mm, a > 1)$	Unidirectional	[22]
$\propto a^{0.72}(d = 2.5mm, a > 2.7)$	$\propto a^{0.39}(d = 5mm, a > 1)$	$w = 1.2d$	
$\propto a^{0.83}(d = 5mm, a > 2.7)$			

Tabla 2.2: Main experimental results for the final properties of the deposits of the collapse of a granular column made of coarse grains of typical size $d \gtrsim 0.3mm$. In the unidirectional experiments w is the width of the channel.

with the physical observation that for small initial aspect ratio columns, the final height is equal to the initial height: $h_\infty = h_0$.

2.3.   Summary of Numerical Results

Significant advances in the problem of the collapse of a granular column have been achieved using numerical simulations, with results that are comparable both qualitatively and quantitatively, with experimental observations. Among the several techniques for studying the problem numerically, one of the most useful is the family of methods known generically as the Discrete Element Method (DEM) which will be discussed in detail in the next chapter. This particular method is convenient because it gives access to all the information of the system at each time step.

Results from numerical simulations [22, 39, 46] have found values for the scaling exponents that differ slightly from those found experimentally, among other

$h^* = h_\infty/h_0$	w	Reference
$\propto a^{-0.55}(a > 1.5)$	w	[3]
$\propto a^0(a < 0.7)$	w	[25]
$\propto a^{-2/3}(a > 0.7)$		
$\propto a^{-3/5}(a > 1.15)$	w	[28]
$\propto a^{-0.55}(d = 2.5mm, a > 1)$	w	[22]
$\propto a^{-0.61}(d = 5mm, a > 1)$	w=1.2d	

Tabla 2.3: Main results for the final height normalized by the initial height of the column in unidirectional experiments, where. Data is recalculated from Table 2.2.

reasons, because of the approximations used to model granular materials: the use of spherical particles (or disks in two dimensions), the geometric constraints of a 2D configuration and the different values of simulation parameters like the friction coefficient or the elastic properties of the grains, all have an effect in the final numerical value of the scaling exponents [40] that makes it different from the experimental results.

Nevertheless, it has been shown that the scaling laws obtained from numerical simulations are consistent with the experimental results [22, 39, 46] and that it is possible to reproduce exactly the numerical values of the exponents and prefactors when the parameters of the model are tuned appropriately [22]. This is important because it allows a calibration between the numerical model used and the experiments to replicate or simulate, with the assurance that the results obtained numerically are valid.

The advantage of numerical simulations is that complete access to all the information of the system is available, allowing a detailed analysis of the problem. For example, using numerical simulations, the free falling phase of the collapse was quantified [39] and characterized in terms of the value of the parameter a; an energy balance was performed to understand how energy is lost during the process [42, 46] providing some insights into why final properties of the columns scale similarly. These detailed analysis are difficult or impossible to measure experimentally.

Numerical results of the scaling of the final distances have shown that these scale as $\sim \lambda a^\beta$, in accordance to experimental results. As opposed to what experiments suggest, results of numerical simulations appear to depend slightly on the properties of the grains used, specifically on the value of the friction coefficient μ

between grains [46]. Finally, [42] found numerically that the shape of the particle is also irrelevant to the scaling laws and the exponents and pre-factors have numerical values that are still in the range of those experimentally measured.

2.4.   Remarks

The scaling laws of the form

$$x^*, h^* = \lambda a^\beta,$$

for the final distances of the deposits formed by the collapse of a granular column have been consistently observed and confirmed both experimentally and numerically. It is remarkable that these scaling relations hold under a variety of conditions: the way in which the grains are released, how the samples are prepared, changing the substrate on the horizontal surface on which the collapse occurs, whether the collapse is axysimmetric or unidirectional, or even the type of grains used.

In all the experiments the dimensions of the columns are of the order of centimeters, with typical grain size of millimeters (see Table 2.1), therefore the ratio of typical grain size to initial height is of the order of $d/h_0 \sim 10^{-2} - 10^{-3}$, which can be considered small.

All experiments are performed under controlled laboratory conditions of air temperature and humidity, under the gravitational acceleration of Earth, with a nominal value of $g_0 = 9.81 m/s^2$. To our knowledge, no experiments have yet been performed under different gravitational accelerations (e.g. extraterrestrial).

The first experiments were done with different types of materials (see for example Fig. 2.1) with similar values of the friction coefficient (see Table 2.1), which is probably why no effect on this property was observed. Subsequent work showed that the use of grains with different friction properties slightly changed the values of the scaling coefficients λ, but the scaling exponents did not vary considerably [3].

This remarkable and important observation leads to the question of whether the collapses depend or not on the friction properties of the grains comprising the

columns. A partial answer to this question is provided by numerical simulations [22, 39, 40, 42, 46] but the question is still open.

Arguably, the flow properties depend on the friction coefficient between grains, which acts to dissipate energy as the grains remain in contact during motion. The final properties of the deposits characterized by the distances x^*, h^*, clearly depend on the transient flow developed during the collapse, so they must depend on the friction properties of the system. This is discussed further in Chapter 3.

To close this Chapter, different experiments and numerical simulations of the collapse of granular columns have established scaling laws for the final properties of the deposits that depend on the ratio of initial height to width of the columns, and very weakly, or none at all, on other variables that would seem likely to affect the collapse, such as the density, shape or size of the grains.

Using experimental evidence, a mathematical model based on scaling properties of the system is built which contains the discussed scaling laws. The question remains open. What is the mechanism at the grain level that makes the deposits end with similar properties? The theory of self-similarity provides a mathematical framework that allows us to partially answer this question.

CHAPTER 3

SCALING AND SELF-SIMILARITY

The scaling law for the final properties of the emplacements discussed earlier underlie the important property of similarity; two granular columns, each with its own values of h_0, x_0, etc., collapsing under the same horizontal surface may seem like different unrelated events, but in the particular case in which both columns have the same value of the parameter a, i.e.

$$\frac{h_0}{x_0} = \frac{H_0}{X_0}, \tag{3.1}$$

the scaling relations observed experimentally indicate that, in both cases, the final height and run-out distances have the same values:

$$h_\infty^* = H_\infty^* \tag{3.2}$$

$$x_\infty^* = X_\infty^*, \tag{3.3}$$

and the two events are similar.

Recognizing this property of similarity of the collapse of a granular column, suggests that the approach developed in [4, 5] can be applied to study the problem. This Chapter describes this mathematical tool, starting from a method for reducing physical problems to their simplest form known as Dimensional Analysis, at

the heart of which is the concept of similarity [38]. Similarity refers to a transformation of variables in a physical system that reduces the number of independent variables that specify the problem [38] by looking at possible relationships between variables based on their dimensions [7].

When it is possible to write all the governing laws and boundary conditions of a given problem in mathematical form, dimensional analysis provides a way to find similarity solutions by identifying the dimensionless variables that appear in the equations. This is done by means of the fundamental result known as the *Buckingham-Pi Theorem*, presented, without proof, in the first section of this Chapter.

With this result, the concepts of self-similarity of the first and second kind are introduced in the next section, and applied to the problem of the collapse of a granular column, where a mathematical formulation is missing, to give insight into the origin of the scaling laws observed experimentally and numerically.

3.1.   Dimensional Analysis and Self-similarity

Dimensional analysis is a tool relating the dimensions of physical quantities in a meaningful way. Its main result, known as the *Buckingham-Pi Theorem*, provides a way to rewrite a physical equation depending on p physical variables (with dimensions) as an equivalent equation in $m = p - k$ dimensionless parameters, by identifying the dimensionless groups based on the number of fundamental units k (for example mass, length and time).

Consider, as an example, the problem of finding the period T of small oscillations of a simple frictionless pendulum (Fig. 3.1). Assume a relation exists between the period T, the length L, the mass M and the acceleration due to gravity on the surface of the Earth g, which has units of length divided by squared time, such that

$$T = f(L, M, g). \tag{3.4}$$

Three fundamental physical units can be identified so that $k = 3$: time t, length l, and mass m, from the list of three physical variables ($p = 3$) L, M and g on which the quantity of interest depends on. The units of the dimensional variables are
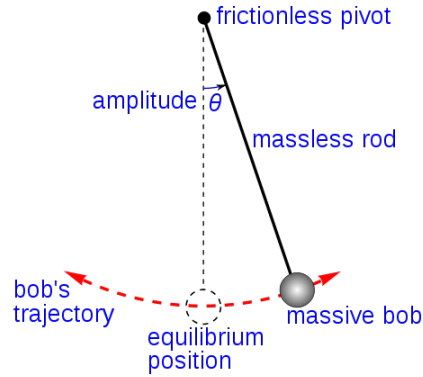
Figura 3.1: The simple pendulum. Image from http://en.wikipedia.org

$$T = [t]; \quad L = [l]$$
$$M = [m]; \quad g = [lt^{-2}].$$

Expressing the dimensions of T as products of powers of the dimensions of L, M and g as $[T] = [L]^{a_1}[M]^{a_2}[g]^{a_3}$, for some values a_1, a_2, a_3, we find that

$$[T] = [L]^{a_1}[M]^{a_2}[g]^{a_3}$$
$$\Leftrightarrow$$
$$t = l^{a_1} m^{a_2} (lt^{-2})^{a_3}$$
$$= l^{a_1+a_3} m^{a_2} t^{-2a_3}$$
$$\Leftrightarrow$$
$$a_1 + a_3 = 0$$
$$a_2 = 0$$
$$-2a_3 = 1$$

so that $a_1 = 1/2, a_2 = 0, a_3 = -1/2$ and thus

$$[T] = [L]^{1/2}[M]^0[g]^{-1/2}.$$

We can construct a single dimensionless quantity Π as

$$\Pi = \frac{T}{(L/g)^{1/2}}$$

such that relation 3.4 is, in dimensionless form

$$\Pi = const. \tag{3.5}$$

The fact that the right hand side of the last expression is a constant follows from the fact that there are $p = 3$ physical governing parameters (L, M, g) and $k = 3$ parameters with independent dimensions (t, l, m), so that, according to the *Buckingham-Pi Theorem*, the number of remaining dimensionless parameters becomes $m = p - k = 3 - 3 = 0$. Relation 3.5 implies that

$$T = const \sqrt{L/g}$$

for the period of small oscillation of a simple pendulum. Dimensional analysis does not give any information on the numerical value of the constant. A detailed analysis of the problem shows that its value is 2π.

3.1.1.   The Buckingham-Pi Theorem

We now sate the *Buckingham-Pi Theorem*, using the previous example as a reference. The statement of the theorem comes from the principle that any physical law must be dimensionally homogeneous, that is, true and valid independent of the size of the base of units used. The theorem tells us that any complete physical equation will, in an appropriate dimensionless form, reduce the number of independent quantities in the problem.

The theorem can be stated as follows [5]: "A physical relationship between some dimensional quantity and several dimensional governing parameters, can be written as a relationship between a dimensionless parameter and several dimensionless products of the governing parameters; the number of dimensionless products m equals the total number of governing parameters p minus the number of governing parameters with independent dimensions k".

A set of parameters $a_1, \ldots, a_k$ has independent dimensions if none of them has a dimension function that can be represented as a product of the dimensions of the others. This set of independent quantities is not unique; consider the simple pendulum example: a complete set of quantities with independent dimensions is comprised of $\{M, L, T\}$ because the dimensions of g can be obtained from a

combination of the others as $[g] = [M]^0[L]^1[T]^{-2}$, but another complete set can be $\{M, L, g\}$ because the dimensions of T can be obtained as $[T] = [M]^0[L]^{1/2}[g]^{-1/2}$.

In general, relationships among quantities that characterize the phenomenon are obtained in the form

$$y = f(a_1, a_2, a_3, \ldots, a_k, b_1, \ldots, b_m), \tag{3.6}$$

where y is the quantity being determined (for example, the period of small oscillations of the simple pendulum T), and its $p = k + m$ arguments

$$a_1, a_2, a_3, \ldots, a_k, b_1, \ldots, b_m$$

are assumed to be given. These are called the governing parameters [4, 5], and are divided into k parameters $a_1, a_2, a_3, \ldots, a_k$ that have independent dimensions, while the dimensions of the m parameters $b_1, \ldots, b_m$ can be expressed as products of powers of the dimensions of the parameters $a_1, a_2, a_3, \ldots, a_k$:

$$[b_1] = [a_1]^{p_1} \cdots [a_k]^{r_1}$$
$$\vdots$$
$$[b_i] = [a_1]^{p_i} \cdots [a_k]^{r_i}$$
$$\vdots$$
$$[b_m] = [a_1]^{p_m} \cdots [a_k]^{r_m}$$

If the dimensions of all the governing parameters are independent, then $m = 0$ and $p = k$; this is the case of the simple pendulum example. In general $k, m > 0$.

The dimension of the quantity to be determined must be expressible in terms of the dimensions of the governing parameters with independent dimensions $a_1, a_2, a_3, \ldots, a_k$ as

$$[y] = [a_1]^p \cdots [a_k]^r.$$

In the simple pendulum example we have $[T] = [M]^p[L]^q[g]^r$. Introducing the

parameters

$$\Pi = \frac{y}{a_1^p \dots a_k^r}$$

$$\Pi_1 = \frac{b_1}{a_1^{p_1} \dots a_k^{r_1}}, \quad \dots, \quad \Pi_i = \frac{b_i}{a_1^{p_i} \dots a_k^{r_i}}, \quad \dots,$$

$$\Pi_m = \frac{b_m}{a_1^{p_m} \dots a_k^{r_m}},$$

where the exponents are chosen such that all the parameters $\Pi, \Pi_1, \dots, \Pi_m$ are dimensionless we can write

$$\Pi = \frac{f(a_1, a_2, a_3, \dots, a_k, b_1, \dots, b_m)}{a_1^p \dots a_k^r}$$

$$= \frac{1}{a_1^p \dots a_k^r} f(a_1, a_2, a_3, \dots, a_k, \Pi_1 a_1^{p_1} \dots a_k^{r_1}, \dots, \Pi_m a_1^{p_m} \dots a_k^{r_m}).$$

so that

$$\Pi = F(a_1, a_2, a_3, \dots, a_k, \Pi_1 \dots, \Pi_m)$$

for a certain function F. It follows, from the principle of dimensional homogeneity of the physical laws, that the function F *must* be independent of the arguments $a_1, a_2, a_3, \dots, a_k$ [4, 5, 38] and can be written in terms of a function Φ of m arguments

$$\Pi = \Phi(\Pi_1 \dots, \Pi_m), \tag{3.7}$$

from which it follows that the relationship for y can be written in terms of a function with a smaller number of variables:

$$y = f(a_1, a_2, a_3, \dots, a_k, b_1, \dots, b_m) = a_1^p \dots a_k^r \Phi \left(\frac{b_1}{a_1^{p_1} \dots a_k^{r_1}}, \dots, \frac{b_m}{a_1^{p_m} \dots a_k^{r_m}} \right), \tag{3.8}$$

which is the statement of the *Buckingham-Pi Theorem*. Self-similar solutions can be derived using dimensional analysis when a mathematical model of the problem is available. In Chapter 5 we apply dimensional analysis to a simple mathematical model for the collapse of a granular step to show this. In what follows of this Chapter, the concepts of self-similarity of the first and second kind are discussed.

3.1.2.   Self-similarity of the first and second kind

Consider Eqn. 3.7,

$$\Pi = \Phi(\Pi_1 \ldots, \Pi_m),$$

and suppose that when Π_m is very small, the limit of the function Φ exists and is finite and non-zero. Then

$$\Phi_0(\Pi_1 \ldots, \Pi_{m-1}) = \lim_{\Pi_m \to 0} \Phi(\Pi_1 \ldots, \Pi_m),$$

defines a new function Φ_0 of one less argument, but more importantly, if it is true that

$$\lim_{\Pi_m \to 0} \Phi(\Pi_1 \ldots, \Pi_m) = \Pi, \tag{3.9}$$

i.e., if the limit exists, we see that the influence of the parameter Π_m, and thus of the corresponding dimensional parameter b_m, on the phenomenon of interest is negligible as $b_m \to 0$, and can be ignored from the list of governing parameters, replacing Φ by a function of one less parameter Φ_0.

When this situation occurs, it is said that the phenomenon has a complete self-similarity, or self-similarity of the first kind with respect to the dimensionless parameter Π_m [4, 5]. A similar conclusion is reached if the limit of Φ exists and is non-zero when the considered parameter is very large.

On the other hand, if

$$\lim_{\Pi_m \to 0} \Phi \quad \text{or} \quad \lim_{\Pi_m \to \infty} \Phi$$

vanish or diverge, the dimensional parameter b_m is essential to the phenomenon and we cannot ignore it from the list of governing parameters. In this case Φ can not be directly replaced by a function with one less argument. Yet, it may be possible to simplify the problem. If we can write

$$\Phi = \Pi_m^{\alpha} \Phi_1(\Pi_1 \ldots, \Pi_{m-1}) + h.o.t., \tag{3.10}$$

even when $\Pi_m \to 0$ (or $\Pi_m \to \infty$), where the higher order terms *h.o.t.* vanish for sufficiently large or small Π_m, then we have that

$$\Phi_1 = \Pi \cdot \Pi_m^{-\alpha} = \frac{y}{b_m^{\alpha} a_1^{p - \alpha p_m} \ldots a_k^{r - \alpha r_m}} = \Pi^*, \tag{3.11}$$

where Φ_1 depends on one less argument, but the parameter b_m remains essential, as it appears in Π^*. The form of Π^* cannot be obtained by dimensional analysis, as it depends on the value of the exponent α. In this case, if it is possible to express Φ_1 as in Eqn. 3.11, the phenomenon is said to have a self-similarity of the second kind with respect to Π_m [4, 5].

Notice that Eqn. 3.11 is a special case of the more general expression

$$\Pi = \Pi_m^\alpha \Phi_1 \left(\frac{\Pi_1}{\Pi_m^{\alpha_1}}, \ldots, \frac{\Pi_{m-1}}{\Pi_m^{\alpha_{m-1}}} \right) \tag{3.12}$$

when all the exponents $\alpha_i = 0, i = 1, \ldots, m - 1$. With this method for reducing the number of arguments for the function describing the phenomenon, the dependence on the essential parameter b_m appears as a power law.

The same procedure can be applied with any dimensionless parameter Π_i of the list for which the limit exists when large or small values are considered. In the next section we will discuss the implications of these assumptions for the problem of the collapse of a granular column.

3.2.   Dimensional analysis of the collapse of a granular column

To conclude this Chapter, the formalism of dimensional analysis and self-similarity of the first and second kind described previously is applied in the problem of the collapse of a granular column, which despite its simplicity, depends on many governing parameters.

As experiments have shown, not all of considered parameters seem to be relevant to the results obtained. In particular, the final run-out and the final height of the emplacements depend only on the initial aspect ratio of the column, and seem to be independent of, e.g., the substrate over which the collapses occur, the density of the material used or the size and shape of the grains, at least when the shape is not extremely aspherical, as in [12, 15].

The final properties of a deposit resulting from the collapse of a column depend on the characteristics of the developed flow during the emplacement formation.

In the remainder of this thesis, attention will focus on the maximum height of the deposit h_m, obtained from the height profile of the emplacements $h = h(x, t)$ at $x = 0$, assuming they are symmetric. Therefore $h_m = h_m(t) = h(0, t)$.

The physical quantities on which the function describing the height profile $h(x, t)$ depends, are assumed to be relevant only at the flow scale and not at the grain scale. Under this assumption, the normal and shear stresses affecting the flow can be approximated based on the arguments given in [42]. The height profile of the deposits as the collapse occurs is likely influenced by the following variables:

x : Spatial coordinate, unidirectional flow;

t : Time;

ρ : Density of the granular material;

d : Typical size of the grains used;

σ : Macroscopic externally imposed shear stress due to the flow;

P : Macroscopic externally imposed normal stress due to the self weight of the
column during flow;

$\dot{\gamma}$: Macroscopic externally imposed deformation rate due to the flow;

g : Local gravitational acceleration;

μ_g : Inter-granular friction;

h_0, x_0 : Initial conditions.

The inter-granular friction coefficient μ_g, is a dimensionless scalar value that describes the ratio of the force of friction with the force that presses together two grains in contact. It is described, at the grain level, according to a Coulomb friction model: $f_t = \mu_f f_n$. A different coefficient of friction that describes the global friction properties of the flow can be defined as the ratio of the macroscopic shear stress to the macroscopic normal stress as

$$\mu_{eff} = \frac{\sigma}{P}. \tag{3.13}$$

The final height of the deposit, i.e. the maximum height after the collapse occurs and grains have stopped their motion, can be seen as the limit

$$h_\infty = \lim_{t \to \infty} h_m(t).$$

The steps for applying dimensional analysis require us to write, for the maximum height of the emplacement

$$h_m(t) = H(t, g, d, \rho, \sigma, P, \dot{\gamma}, h_0, x_0, \mu_g). \tag{3.14}$$

Equation 3.14 is written based on the experimental and numerical evidence discussed throughout this thesis. The quantity of interest, the maximum height of the emplacement h_m, depends on $p = 10$ governing variables. We choose the $k = 3$ variables with independent dimensions h_0, P, g. According to the *Buckingham-Pi Theorem*, we can express it as a dimensionless function of $m = p - k = 7$ parameters:

$$\Pi = \frac{h_m}{h_0}$$

$$\Pi_1 = \frac{t}{\sqrt{h_0/g}}$$

$$\Pi_2 = \frac{\rho g h_0}{P} \qquad\qquad \Pi_3 = \frac{d}{h_0}$$

$$\Pi_4 = \frac{\sigma}{P} \qquad\qquad \Pi_5 = \frac{\dot{\gamma}}{\sqrt{g/h_0}}$$

$$\Pi_6 = \frac{x_0}{h_0} \qquad\qquad \Pi_7 = \mu_g,$$

so that

$$\Pi = \Psi\left(\Pi_1, \Pi_2, \Pi_3, \Pi_4, \Pi_5, \Pi_6, \Pi_7\right), \tag{3.15}$$

describes, in dimensionless form, the maximum height of the deposit as the collapse occurs.

3.2.1.   Evolution of the maximum height

The evolution of the normalized maximum height of the deposit, Eqn. 3.15, can be expressed as

$$h_m^* = \Psi \left(\tau, a, \frac{d}{h_0}, \frac{\sigma}{P}, \frac{\rho g h_0}{P}, \frac{\dot{\gamma}}{\sqrt{g/h_0}}, \mu_g \right). \tag{3.16}$$

As noted before, the ratio of the shear stress σ to the normal confinement macroscopic stress P can be seen as an effective macroscopic coefficient of friction for the flow, $\mu_{eff} = \sigma/P$.

In the case that $\rho g h_0 / P \ll 1$ or $\rho g h_0 / P \gg 1$, it can be assumed that the maximum height of the deposit has a self-similarity of the second kind on this dimensionless parameter, allowing us to write

$$h_m^* = \left[\frac{\rho g h_0}{P} \right]^\alpha \Psi_1 \left(\frac{\tau}{\left[\frac{\rho g h_0}{P} \right]^{\alpha_0}}, \frac{a}{\left[\frac{\rho g h_0}{P} \right]^{\alpha_1}}, \frac{d/h_0}{\left[\frac{\rho g h_0}{P} \right]^{\alpha_2}}, \frac{\mu_{eff}}{\left[\frac{\rho g h_0}{P} \right]^{\alpha_3}}, \frac{\mu_g}{\left[\frac{\rho g h_0}{P} \right]^{\alpha_4}}, \frac{\frac{\dot{\gamma}}{\sqrt{g/h_0}}}{\left[\frac{\rho g h_0}{P} \right]^{\alpha_5}} \right).$$

Further, assume that the self-similarity exponents are such that $\alpha_0 = \alpha_1 = \alpha_2 = \alpha_3 = \alpha_4 = 0$ therefore

$$h_m^* = \left[\frac{\rho g h_0}{P} \right]^\alpha \Psi_1 \left(\tau, a, \frac{d}{h_0}, \mu_g, \mu_{eff}, \frac{\frac{\dot{\gamma}}{\sqrt{g/h_0}}}{\left[\frac{\rho g h_0}{P} \right]^{\alpha_5}} \right).$$

If the remaining scaling exponents are related as $\alpha - \alpha_4 = 1/2$, the combination of dimensionless parameters

$$\left[\frac{\rho g h_0}{P} \right]^\alpha \cdot \frac{\frac{\dot{\gamma}}{\sqrt{g/h_0}}}{\left[\frac{\rho g h_0}{P} \right]^{\alpha_5}}$$

reduces to

$$\frac{h_0 \dot{\gamma}}{\sqrt{P/\rho}},$$

and the dependence on gravity only appears in the dimensionless time τ. There-

fore, we can write, for the maximum height

$$h_m^* = \Psi_1 \left(\tau, a, \frac{d}{h_0}, \frac{h_0 \dot{\gamma}}{\sqrt{P/\rho}}, \mu_{eff}, \mu_g \right). \tag{3.17}$$

Notice that there is no *a priori* reason why the scaling exponents should have these values. They are just selected for convenience.

Recently, significant advances have been reached in the rheological description of granular flow [13]. A single dimensionless number, the inertial number I, has been used to describe flow properties, in particular for the transient flow in the column collapse problem [21, 23]. The inertial number I can be interpreted as the ratio of two time scales at the grain level, $I = t_P/t_D$, where $t_D = \dot{\gamma}^{-1}$ is the time that one layer of material takes to move over a distance d with respect to another, and $t_P = d\sqrt{\rho/P}$ is the time needed by the top layer to be pushed back to its lower position after climbing over another grain [13], so that

$$I = \frac{\dot{\gamma} d}{\sqrt{P/\rho}}.$$

This number characterizes the nature of the flow into a quasi-static regime, when $I \to 0$; a dense regime, when $10^{-2} < I < 10^{-1}$; and a collisional regime, for $I > 10^{-1}$. Together with the inertial number, an effective friction coefficient μ_{eff} for the flow can be constructed, as defined previously, as the ratio of deformation to normal stresses.

It has been observed that this effective friction is constant during the quasi-static regime ($I1$), while it increases with I and thus is no longer constant in the dense regime, indicating a shear rate dependent regime [13]. It is argued that a unique relationship between the effective friction coefficient of the flow $\mu_{eff} = \sigma/P$ and the number I exists at the grain scale,

$$\frac{\sigma}{P} = \mu_{eff}(I),$$

that describes average flow properties like volume fraction, velocity profiles and effective friction [13]. Noticing that

$$\frac{h_0 \dot{\gamma}}{\sqrt{P/\rho}} = I \cdot \frac{h_0}{d}$$

in Eqn.3.17, and assuming a unique relation between this number I and the effective friction of the flow, we can write

$$h_m^* = \Psi_1 \left(\tau, a, \frac{d}{h_0}, \mu_{eff}, \mu_g \right) \tag{3.18}$$

$$\mu_{eff} = \mu_{eff}(I), \tag{3.19}$$

for the final height. Note that the explicit dependence on I has been absorbed into the rheological description of the flow given by $\mu_{eff} = \mu_{eff}(I)$. In all experiments and numerical simulations, the ratio of the typical grain size to the initial height of the column is of the order of $d/h_0 \sim 10^{-1}$ (see Table 2.1), so we can write Eqn. 3.18 as

$$h_m^* = \Psi_0 \left(\tau, a, \mu_{eff}, \mu_g \right) \tag{3.20}$$

$$\mu_{eff} = \mu_{eff}(I), \tag{3.21}$$

where $\Psi_0 = \lim_{d/h_0 \to 0} \Psi_1$. From the experimental settings of the problem the influence of the dimensionless parameter d/h_0 is negligible. In terms of the discussion following Eqn. 3.9, *the final normalized height of the deposits has a self similarity of the first kind on the parameter d/h_0.*

The number I can be defined locally for homogeneous simple granular flows, but in the collapse of a granular column it is difficult to determine it locally due to the transient nature of the flow [21, 23]. Nevertheless, a macroscopic equivalent to the inertial number can be constructed [42] comparing two macroscopic time scales, to obtain

$$I = \frac{d_{eff}(x - x_0)^{3/2}}{h - h_0} \frac{1}{t\sqrt{c_0 A g}}, \tag{3.22}$$

where d_{eff} is an effective grain diameter, equal to the typical diameter d of the grains in a mono-disperse column, and $c_0 A$ is the initial 2D area occupied by the compacted grains in the column. The details leading to Eqn. 3.22 can be found in [42] and go as follow: in the flowing phase of a collapsing column, a horizontal deformation is experienced such that the rate of deformation of the deposit can be approximated as

$$\dot{\gamma} \sim \frac{x(t) - x_0}{t} \frac{1}{h_0 - h(t)}.$$

A characteristic time T_P can be constructed from the pressure of the whole column

at the base $P = \frac{Mg}{x-x_0}$, where M is the total mass of the column, g the acceleration due to gravity and x is the extension of the deposit, as

$$T_P = d\frac{(x - x_0)^{1/2}}{\sqrt{c_0 Ag}},$$

where $c_0 A$ is the initial 2D area. Comparing the pressure time scale with the effective shear rate, the inertial number I shown above is obtained. As it has been discussed by others, large values of I indicate that the pressure of the material above dominates over horizontal deformation of the deposit, as expected for short times. As time advances, I decreases as the shear deformation becomes important.

3.2.2. The final height of the deposit

In the previous section we found that the dimensionless function given by Eqn. 3.20

$$h_m^* = \Psi_0\left(\tau, a, \mu_{eff}, \mu_g\right)$$

together with the rheological empirical law $\mu_{eff} = \mu_{eff}(I)$ describe, in principle, the evolution of the maximum height of the deposits in terms of 4 dimensionless parameters. The final height of the deposit h_∞ can be found from Eqn. 3.20 taking the appropriate limit in the time variable:

$$h_\infty^* = \lim_{\tau \to \infty} h_m^*. \tag{3.23}$$

This limit exists and is finite, because all emplacements reach a measurable final height. The final height can thus be seen as a function of 4 dimensionless parameters a, μ_{eff}, μ_g, I expressed as

$$h_\infty^* = \Phi_0\left(a, \mu_{eff}, \mu_g\right) \tag{3.24}$$

$$\mu_{eff} = \mu_{eff}(I), \tag{3.25}$$

where $\Phi_0 = \lim_{\tau \to \infty} \Psi_0$. Assuming a self-similarity of the second type when the parameter $a \to 0$ or $a \to \infty$ gives

$$h_\infty^* = a^\beta \Phi_1\left(\frac{\mu_{eff}}{a^{\beta_0}}, \frac{\mu_g}{a^{\beta_1}}\right) \tag{3.26}$$

for the final height of the deposit. Again, no information on the values of the self-similar exponents β_i is available. They have to be evaluated either by experiments or numerical simulations. Assuming $\beta_0 = \beta_1 = 0$ simplifies Eqn. 3.26 to

$$h_\infty^* = a^\beta \Phi_2 \left(\mu_{eff}, \mu_g \right).$$

This last expression coincides with [26], with the additional result of the power law scaling on the initial aspect ratio a recovering the experimentally observed scaling law for the final height of the deposit.

3.3. Conclusions and remarks

This Chapter has described the general ideas of dimensional analysis, scaling and self-similarity of the first and second kind for general systems. When applied to the problem of the collapse of a granular column, it is found that the height of the deposit depends on at least $p = 10$ governing parameters. Using dimensional analysis this can be reduced to $m = 7$ dimensionless parameters. The dimensionless final height, obtained when the grains stop moving after very long times, can be described using a function of $m = 5$ dimensionless parameters, while the evolution of the maximum height still depends on the $m = 7$ arguments.

Assuming that a self-similarity of the second kind exists for the maximum height when the pressure of the column is large compared to its own weight and that the effect on gravity only occurs on the time variable, can lead to a function that depends on the inertial number via a local rheology, as proposed by some authors [13], of the form $\mu_{eff} = \mu_{eff}(I)$. This function also depends on the initial aspect ratio as a power law, Eqn. 3.26, if self-similarity of the second kind is assumed. The numerical values of the scaling exponents are unknown, but they can be evaluated by means of experimental results or numerical simulations.

Experimental considerations show that these functions have a self-similarity of the first kind on the ratio of typical grain size to initial height of the column d/h_0. Once the collapse ends, the assumption of self similarity of the second kind, in the limit of small or large initial aspect ratio, of the column leads to the power law scaling of the final height scaling with this parameter, Eqn. 3.26, as a function that depends on the frictional properties of the material.

In the remainder of this work we present results of numerical simulations of the collapse of granular columns to test the validity of the hypothesis of self-similarity discussed in this Chapter. The next Chapter describes the numerical method used to perform the simulations and the parameters used to obtain the results, which are reported in Chapter 6, where we study the effect of varying the shape of the grains used to make the column, and Chapter 7, where the effect of varying the value of the local gravitational acceleration is studied. Before such results are presented, in Chapter 5 we show how a mathematical setting of the problem allows the construction of self-similar solutions from a simple model used to describe granular flow.

CHAPTER 4

NUMERICAL METHOD

There are many different numerical methods for the simulation of granular media (see for example [34] for a comprehensive review) and each has its advantages and disadvantages. Since granular materials are collections of many individual particles, with sizes ranging from micrometers to centimeters, one suitable method to perform simulations of this type is the Discrete Element Method (DEM).

This method consists in the numerical integration of the equations of motion, as given by Newton's laws, for each of the particles making up the granular medium and is the subject of this Chapter. We start by a description of the model for granular materials used in the numerical simulations, followed by the numerical algorithm used to integrate the equations of motion.

A grain is modeled as a spherical(disk) particle of radius R in 3(2) dimensions. This way of modeling granular particles is the simplest possible and allows us to express the interactions in terms of quantities related to the geometry properties of the particles. The location in space of a grain of typical size R_i and mass m_i is determined by a position vector $\mathbf{r}_i = (x_i, y_i, z_i)$ with $z_i = 0$ in 2 dimensions.

The dynamics of N grains located at the positions

$$\mathbf{r}_i, i = 1, \cdots, N$$

is governed by $3N$ time dependent coupled equations given by Newton's Second Law:

$$\ddot{\mathbf{r}}_i = \frac{\mathbf{f}_i(r_{ij}, v_{ij})}{m_i} \tag{4.1}$$

$$\tau_i = I_i \dot{\omega}_i \tag{4.2}$$

where $\mathbf{f}_i$ and τ_i are the total force and the net torque acting on the *ith* particle (radius R_i, mass m_i, moment of inertia I_i) due to all the *jth* particles that interact with it. The force that gives rise to the linear and angular accelerations $\ddot{\mathbf{r}}_i$ and $\dot{\omega}_i$ is an explicit function of the relative position and velocity of the interacting particles:

$$r_{ij} = |r_i - r_j| \tag{4.3}$$

$$v_{ij} = |v_i - v_j|. \tag{4.4}$$

In general, the $3N$ nonlinear coupled equations given by 4.1 can not be solved analytically and numerical solutions must be sought. The numerical method which calculates the forces (and torques) and integrates Eqns. 4.1 to obtain the trajectories of every particle in the system, is known as the Discrete Element Method (DEM) [34]. Unlike the classical Molecular Dynamics calculations [1, 35], in the DEM for granular media, interactions are short ranged and only occur when the particles are in contact.

Two grains interact if the distance from their centers is less than the sum of their radii. In other words, if a positive relative overlap between grains occurs, then there is force between them, otherwise the force is zero. The total force $\mathbf{f}_i$ on the *ith* grain is the sum of all pairwise interactions with the rest of the grains that are in contact:

$$\mathbf{f}_i = \sum_{i \neq j} \mathbf{f}_{ij}(r_{ij}, v_{ij}). \tag{4.5}$$

The interaction law between the grains, i.e. the explicit functional form of the pairwise forces $\mathbf{f}_{ij}(r_{ij}, v_{ij})$ in Eqn. 4.5, is determined by the so-called contact model. Before discussing it, the numerical algorithm implemented to integrate the system given by Eqn. 4.1 is described.

4.1.   Integration algorithm

The numerical integration of the equations of motion Eqn. 4.1 for the translational degree of freedom is done using an algorithm known as the Velocity-Verlet method is used [1, 2, 41]. This method approximates the solution to the second order differential equation for the *ith* grain, at the discrete time $t_{k+1} = (k+1)dt$ using a non-zero step size dt, from the information at the previous time $t_k = kdt$, according to the following rule:

$$r_i^{k+1} = r_i^k + dtv_i^k + dt^2 \frac{f_i^k}{2m_i} \tag{4.6}$$

$$v_i^{k+1} = v_i^k + dt\frac{f_i^k + f_i^{k+1}}{2} \tag{4.7}$$

where we have used the notation

$$X_i^k = X_i(t_k) = X_i(kdt)$$

for the value of the dynamical variable X_i at the *kth* time step. Note that the numerical method requires the value of the force at a future time step $t_{k+1} = (k+1)dt$, therefore to be able to use this algorithm, the explicit functional form of the force has to be known in advance; this is known as the contact model and will be discussed next.

4.2.   Contact Model

The functional form of the interaction between grains when they are in contact is needed for the numerical algorithm described previously. The contact model provides an expression for these forces when grains are interacting. No model can completely describe all the possible interactions occurring when two (or more grains) are in contact during grain motion. All models are restricted and limited by the assumptions leading to them, and the best possible model depends on the problem to be solved.

The simplest model, and the one used in this work, is that in which grains can be represented as spheres (in 3 dimensions) or disks (in 2 dimensions) that interact
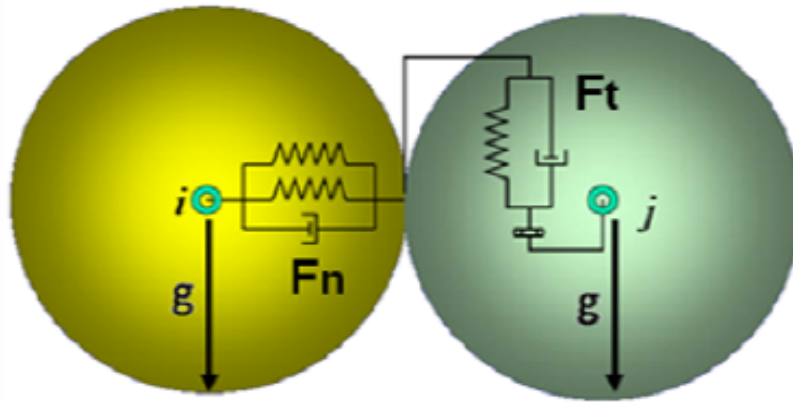
Figura 4.1: Schematic diagram of interaction forces during mechanical contact.

only at mechanical contact. Mechanical contact is defined in terms of the distance between the centers of mass of the interacting grains: two grains with radius R_i, R_j located at the positions given by the vectors $\mathbf{r_i}, \mathbf{r_j}$ are in mechanical contact if

$$\xi_{ij} = R_i + R_j - r_{ij} > 0, \tag{4.8}$$

where $r_{ij} = |\mathbf{r}_{ij}| = |\mathbf{r}_i - \mathbf{r}_j|$ is the relative distance between the positions of the grains. The quantity ξ_{ij} defined by Eqn. 4.8 measures the relative overlap of interacting grains and is sometimes referred to as the compression. When mechanical contact exists between two grains, the force is nonzero and acts to prevent further overlap and to break off the contact i.e., the force is of the form of a repulsive spring with a magnitude that explicitly depends on the compression: as the compression between grains increases, so does the repulsive force.

This simple interaction models the physical effect of an elastic deformation around the point of contact on the surface of the grains. The elastic deformation is accompanied with a loss of energy during the contact, a fundamental characteristic of granular media which are highly dissipative systems.

The interaction between grains in mechanical contact is divided into two mutually orthogonal components in the normal ($\hat{n}$) and tangential ($\hat{t}$) direction relative to the line joining their centers as shown schematically in Fig. 4.1.

Ignoring the force due to the acceleration of gravity, the force acting between par-

ticles that are in mechanical contact can be expressed as:

$$\mathbf{f}_{ij} = \begin{cases} f_{ij}^n \hat{n} + f_{ij}^t \hat{t} & \text{if } \xi_{ij} > 0 \\ 0 & \text{otherwise} \end{cases}, \tag{4.9}$$

where $f_{ij}^n(f_{ij}^t)$ is the magnitude of force in the normal (tangential) direction acting on the *ith* grain due to the interaction with *jth* grain, with which it is in mechanical contact. The force in the normal direction causes a change in the translational degree of freedom, while the tangential force causes a change in the rotational degree and in the translational degrees of freedom.

The force in the normal direction acts as a spring modeling elastic deformation and preventing further overlap of the grains and dissipates energy. This is achieved with an elastic contact force that depends on the normal compression ξ_{ij}^n, and a damping force proportional to the normal relative velocity v_{ij}^n of the grains. In the tangential direction a shear elastic and damping force proportional to the tangential overlap ξ_{ij}^t, and relative velocity v_{ij}^t respectively is implemented. Altogether the interaction contact model can be written as:

$$f_{ij}^n = k_n \xi_{ij}^n - \gamma_n v_{ij}^n \tag{4.10}$$

$$f_{ij}^t = k_t \xi_{ij}^t - \gamma_t v_{ij}^t. \tag{4.11}$$

Friction is implemented via a Coulomb type model, characterized by a friction coefficient μ_g, such that

$$f_{ij}^t \leq \mu_g f_{ij}^n, \tag{4.12}$$

i.e., the tangential force grows according to the model 4.11 until $f_{ij}^t / f_{ij}^n = \mu$ and is then maintained at $f_{ij}^t = \mu_g f_{ij}^n$ until the grains lose contact.

The interaction model described by Eqns. 4.10 and 4.11 is referred to as a "spring-dashpot" model due to the form of the elastic and damping terms. The elastic and viscoelastic constant coefficients k_n, k_t and γ_n, γ_t are calculated from material properties according to formulas that depend on the masses, the radii, the restitution coefficient and Young's and shear moduli, and together are known as the Hertz or Hooke contact model [20].

In this work we used the Hertz contact model, in which the elastic coefficient k_n depends non-linearly on the compression ξ_{ij}^n as $\propto \sqrt{\xi_{ij}^n}$, compared to the Hooke
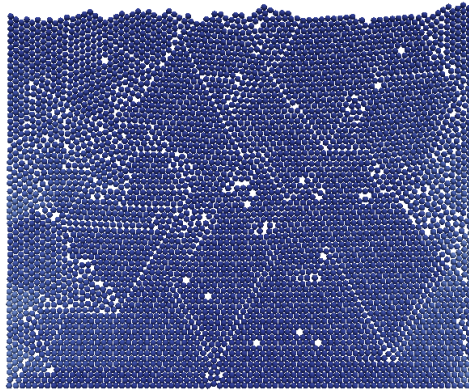
Figura 4.2: Typical initial state of the system. $a = 1.6, g = 9.81m/s^2$.

case in which the normal force is linear in the compression.

4.3. Simulation Parameters

In this study the Hertz contact model, described in the previous section, is used to simulate the collapse of granular columns in a quasi-2D configuration. Grains are modeled as spheres of uniform density $\rho = 2500kg/m^3$ with a constant diameter $d = 0.9mm$, a restitution coefficient of $e = 0.5$, a Young's modulus of $Y = 4.0 \times 10^6 Pa$ and a Poisson ratio equal to $\nu = 0.5$. These values, typical of glass beads used in the laboratory, are fixed in all the numerical simulations. The friction coefficient value μ is the same for all the grains on a given column, and is varied between $[0.5, 0.95]$. Interaction with the walls before the collapse begins is modeled with the same Hertz contact model, considering the walls as having the same material and friction properties.

Columns are constructed by pouring $N_t = 5000$ grains initially at random positions into a rectangular region defined by walls whose half separation determines the initial width x_0 of the column, and a depth equal to one diameter. As shown in Fig. 4.2, grains are confined such that the system is essentially in 2 dimensions. The walls holding the grains in the direction perpendicular to the reading plane are such that the values of μ, γ_n, γ_t are all equal to zero so that no dissipation with these walls occur and they only act as holding planes for the grains in the corresponding direction.

Tabla 4.1: Parameter values used for the simulations. The inter-granular friction coefficient μ and the value of gravity are changed for each column of initial aspect ratio a, defined in the main text. ($g_0 = 9.81 m/s^2$).

μ:	0.5	0.55	0.6	0.65	0.7	0.75	0.8	0.85	0.9	0.95
a:	22.53	14.63	5.75	4.55	3.70	3.08	2.58	2.20	1.67	1.50
g/g_0:	0.1	0.2	0.3	0.4	0.5	1.0	10.0			

After pouring the grains they are left to settle and reach an equilibrium state. At this moment the grain with the largest vertical position is located to determine the initial height of the column, h_0, and the value of the corresponding initial aspect ratio of the column is obtained as $a = h_0/x_0$. In this way 11 columns with $1.5 \leq a \leq 22.5$ are obtained.
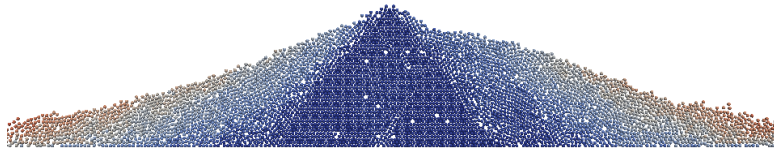

Figura 4.3: State of the column of Fig. 4.2 75 time steps after the walls have been released, $t \sim 0.075s$. Colors indicate the magnitude of the velocity of the grains.

At $t = 0$ the side walls are removed instantaneously, releasing the grains and initiating the collapse. Figure 4.3 shows the state of a typical run after 75 time steps once the walls have been removed, for a column collapsing under Earth's gravity $g = g_0 = 9.81m/s^2$. Finally, for this study the magnitude of the gravitational acceleration under which the collapse occurs is also varied, so that for each column and each value of inter-granular friction, the value of the gravitational acceleration is also changed. We considered fractional multiples of the value of gravity on Earth $g_0 = 9.81m/s^2$, as shown in Table 4.1.

CHAPTER 5

EXAMPLE 1. SHALLOW WATER EQUATIONS MODEL IN ONE DIMENSION

Despite the lack of a theoretical framework, several attempts to model the granular flow of the collapse of a granular column have been conducted [11, 19, 21, 23, 27, 33], but none of them provides full understanding of the nature of the power law behavior observed experimentally [26]. It is possible to understand the power law scaling for the final run-out by means of a dimensional analysis based on the balance between inertia, pressure gradient and frictional forces, under the assumption that the flow is localized on a surface layer and vertical momentum transfers are taken into account [25].

The difficulties of modeling the collapse of a granular column come with the transient nature of the flow. Any model should take into account the transfer of vertical momentum during the downfall of the column at the initial stage of the collapse [25, 27], and a second stage during which material flows over static grains in a layer whose shape varies in time and depends on the initial aspect ratio [25].

A complete modeling of the collapse of a granular column is beyond the objective of this work. Instead we are interested in applying the concepts of self-similarity

and scaling presented earlier in Chapter 3. In this Chapter we present a simple model that has been used with some success to describe the collapse of granular columns [3, 19, 27, 32, 33]. Although the model, known as the shallow-water approximation, is derived under the assumption of negligible vertical momentum transfer and basal friction, it captures some of the observed behavior for small values of a, in particular the run-out distance of the emplacements. The model has also been used as a starting point to model similar events on other planets, like the Valles Marineris landslides of Mars [26, 31, 33].

No formal derivation of the shallow-water equations in one dimension is presented (see [19] for a detail derivation of the model equations), instead they are solved analytically by means of dimensional analysis, constructing a self-similar solution that satisfies the initial and boundary conditions of a finite volume (area) of granular material that starts to flow at $t = 0$ by releasing one of the side walls (see Fig. 5.1).

5.1.   The Shallow Water Equations

The Shallow Water Equations (SWE) is a model obtained by depth averaging the momentum conservation equations [19, 27, 33] under the assumptions that vertical velocities of an incompressible flow of constant density are smaller than the characteristic tangential velocity. In one dimension they are

$$
\begin{aligned}
\frac{\partial h}{\partial t} + \frac{\partial (uh)}{\partial x} &= 0 \\
\frac{\partial u}{\partial t} + u\frac{\partial u}{\partial x} &= -gK\frac{\partial h}{\partial x} + s
\end{aligned}
\tag{5.1}
$$

where u is the depth-averaged horizontal velocity, h the height of the flowing grains and g the acceleration due to gravity. The term gKh_x is proportional to the material slope; K is a constant known as the "Earth pressure coefficient" and represents the ratio between vertical and horizontal normal stresses [19, 25, 27]. Its value depends on the internal friction but does not affect the value of the scaling exponent of the power law dependence [3, 25]. Following [27] we will set its value equal to unity, $K = 1$. The source term s is included as a model for the basal
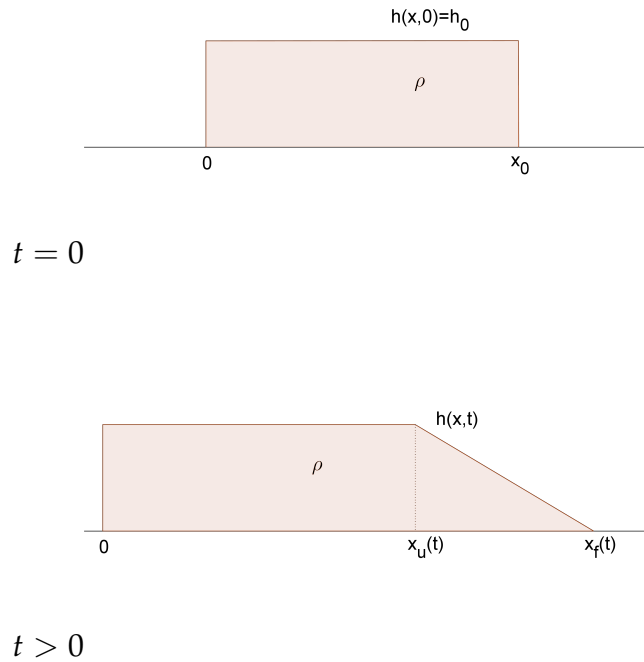
Figura 5.1: Schematic of the flow due to the collapse of a semi-infinite granular column. Classical dam break problem with a granular material.

friction. In this work a Coulomb type friction law

$$s = -g \, \text{tg} \, \delta \text{sgn}(u), \tag{5.2}$$

is used, where sgn defines the sign of u and δ is the internal friction angle (friction coefficient of the granular material). More complex models exist [17, 19] that better capture details of the granular flow, in particular the friction properties of the granular materials, but we keep the simplest possible model which has been used previously [3, 19, 27, 32, 33] with interesting results.

In this chapter the system given by Eqns. 5.1 is used to study the collapse of a granular column in one dimension. The problem is sketched in Fig. 5.1: a mass of granular material of uniform density ρ is placed in a step with initial height h_0 and initial width x_0, so that $a = h_0/x_0 \ll 1$, and left to flow under the action of gravity by removing the right side wall at $t = 0$. The functions $h(x,t)$ and $u(x,t)$ of Eqns. 5.1 give the height and the velocity of the flowing granular mass.

With reference to Fig. 5.1, a fixed impenetrable wall is located at $x = 0$ and the releasing gate is at $x = x_0$, so the following initial and boundary conditions hold:

$$h(x,0) = \begin{cases} h_0 & \text{if } 0 \leq x \leq x_0 \\ 0 & \text{if } x > x_0 \end{cases}; \quad u(x,0) = 0$$

$$h(x_f,t) = \left.\frac{\partial h}{\partial x}\right|_{x=x_f} = 0; \quad u(0,t) = 0 \tag{5.3}$$

$$x_f(0) = x_0; \quad \dot{x}_f(0) = 0,$$

where $x_f(t)$ is the position of the front as the flow moves towards the positive x direction (Fig. 5.1). In this configuration the velocity is always positive, so the basal friction model Eqn. 5.2 becomes

$$s = -g\mu, \tag{5.4}$$

with $\mu = \operatorname{tg}\delta$ is the friction coefficient. The total area, or volume per unit length, of granular material is constant and equal to $A_0 = x_0 h_0 = a x_0^2$.

5.2.   Dimensional analysis and scaling

The mathematical formulation of the problem makes it possible to express the height and the velocity of the flowing grains in terms of the governing parameters. Once the initial width x_0 and height h_0 are specified, the total area of material $A_0 = x_0 h_0$ is fixed by these choices. The value of gA_0 can be used as a governing parameter instead of x_0. Then the height and velocity can be written as

$$h = h(x,t,g,h_0,gA_0,K,\mu)$$

$$u = u(x,t,g,h_0,gA_0,K,\mu). \tag{5.5}$$

There are $p = 7$ governing parameters with dimensions

$$[h] = [x] = [h_0] = L,$$
$$[u] = LT^{-1},$$
$$[t] = T,$$
$$[g] = LT^{-2},$$
$$[gA_0] = L^3 T^{-2}$$
$$[K] = [\mu] = 1.$$

Note that there are only $k = 2$ parameters with independent dimensions (L, T). The results of Chapter 3 tell us that we can express the functions of Eqns. 5.5 in terms of $m = p - k = 7 - 2 = 5$ dimensionless parameters. It is convenient to work with the function gh instead of h itself. By choosing as a complete set of parameters with independent dimensions the pair (gA_0, t), the $m = 5$ dimensionless parameters are

$$\frac{gh}{(gA_0)^{2/3}t^{-2/3}} = \phi(\Pi_1, \Pi_2, \Pi_3, \Pi_4, \Pi_5)$$
$$\frac{u}{(gA_0)^{1/3}t^{-1/3}} = \psi(\Pi_1, \Pi_2, \Pi_3, \Pi_4, \Pi_5)$$
$$\xi = \Pi_1 = \frac{x}{(gA_0)^{1/3}t^{2/3}}$$
$$\Pi_2 = \frac{h_0}{(gA_0)^{1/3}t^{2/3}} \tag{5.6}$$
$$\Pi_3 = \frac{g}{(gA_0)^{1/3}t^{-4/3}}$$
$$\Pi_4 = K$$
$$\Pi_5 = \mu.$$

so that

$$gh = (gA_0)^{2/3}t^{-2/3}\phi(\xi, \Pi_2, \Pi_3, \Pi_4, \Pi_5)$$
$$u = (gA_0)^{1/3}t^{-1/3}\psi(\xi, \Pi_2, \Pi_3, \Pi_4, \Pi_5). \tag{5.7}$$

By plugging the expressions given by Eqns. 5.7 into the shallow water equation, we find the ordinary differential equations for the dimensionless functions ϕ, ψ. Before doing so, a different scaling is presented which reduces the system of Eqns.

5.1 further. Following [3], we introduce the following parameters:

$$\hat{h} = \frac{h}{h_0}$$
$$\hat{x} = \frac{x}{h_0 K \mu^{-1}}$$
$$\hat{u} = \frac{u}{\sqrt{g h_0 K}}$$
$$\hat{t} = \frac{t}{\sqrt{h_0 K / g}},$$

(5.8)

Notice that under these transformations the case $\mu = 0$ must be treated separately, but since we are studying granular materials the friction coefficient is assumed not to vanish. With the scalings given by Eqns. 5.8, the shallow water equations become

$$\frac{\partial \hat{h}}{\partial \hat{t}} + \frac{\partial(\hat{u}\hat{h})}{\partial \hat{x}} = 0$$
$$\frac{\partial \hat{u}}{\partial \hat{t}} + \hat{u}\frac{\partial \hat{u}}{\partial \hat{x}} + \frac{\partial \hat{h}}{\partial \hat{x}} = -1$$

(5.9)

The initial and boundary conditions become

$$\hat{h}(\hat{x},0) = \begin{cases} 1 & \text{if } 0 \le \hat{x} \le \frac{1}{aK\mu^{-1}} \\ 0 & \text{if } \hat{x} > \frac{1}{aK\mu^{-1}} \end{cases} ; \quad \hat{u}(\hat{x},0) = 0$$
$$\hat{h}(\hat{x}_f,\hat{t}) = \left.\frac{\partial \hat{h}}{\partial \hat{x}}\right|_{\hat{x}=\hat{x}_f} = 0; \quad \hat{u}(0,\hat{t}) = 0$$
$$\hat{x}_f(0) = \frac{1}{aK\mu^{-1}};$$

(5.10)

where $aK\mu^{-1}$ is the rescaled initial aspect ratio.

Equations 5.9 with the boundary conditions 5.10 are solved using the self-similar solutions obtained by dimensional analysis, by combining the scalings given by Eqns. 5.7 and 5.8:

$$gh = gh_0\hat{h} = (gA_0)^{1/3} t^{-2/3}\phi(\xi)$$
$$u = (gh_0 K)^{1/2}\hat{u} = (gA_0)^{1/3} t^{-1/3}\psi(\xi),$$

It is found that

$$\hat{h} = \frac{1}{(a^2 K)^{1/3}} \hat{t}^{-2/3} \phi(\xi)$$

$$\hat{u} = \frac{1}{(aK^2)^{1/3}} \hat{t}^{-1/3} \psi(\xi),$$

(5.11)

with the self-similar length scale

$$\xi = \frac{\hat{x}}{\left(\frac{\mu^3}{aK^2} \right)^{1/3} \hat{t}^{2/3}}.$$

(5.12)

The boundary conditions become

$$\hat{h}(\hat{x}_f, \hat{t}) = 0 \Rightarrow \quad \phi(\xi_f) = 0$$

$$\hat{h}_{\hat{x}}(\hat{x}_f, \hat{t}) = 0 \Rightarrow \quad \phi'(\xi_f) = 0$$

$$\hat{u}(0, \hat{t}) = 0 \Rightarrow \quad \psi(0) = 0$$

$$\hat{u}(\hat{x}_f, \hat{t}) = \frac{d\hat{x}_f}{d\hat{t}}$$

(5.13)

Accelerations, given by Π_3 from Eqn. 5.6, transform as

$$\Pi_3 = (aK^2)^{1/3} \hat{t}^{4/3}.$$

(5.14)

Substituting Eqns. 5.11 into Eqns. 5.9, we find the ordinary differential equations satisfied by ϕ, ψ:

$$-\frac{2}{3}(\phi + \xi\phi') + \frac{1}{\mu}(\phi\psi)' = 0$$

$$-\frac{1}{3}\psi - \frac{2}{3}\xi\psi' + \frac{1}{\mu}\psi\psi' + \frac{K}{\mu}\phi' = -\Pi_3,$$

(5.15)

where the prime denotes differentiation with respect to ξ. The solutions ϕ, ψ to Eqns. 5.15 are given in terms of the dimensionless parameters Π_i, according to the analysis described earlier. We now proceed to solve them.

The first of Eqns. 5.15 can be easily written as

$$(\frac{1}{\mu}\phi\psi - \frac{2}{3}\xi\phi)' = 0,$$

(5.16)

which can be integrated directly to give

$$\frac{1}{\mu}\phi\psi - \frac{2}{3}\xi\phi = c_1.$$ (5.17)

Applying the boundary conditions at $\xi = 0$ we find that

$$c_1 = 0$$

and the solution

$$\psi(\xi) = \frac{2\mu}{3}\xi.$$ (5.18)

Substituting this solution into the second of Eqns. 5.15, we are left with

$$\frac{K}{\mu}\phi' = \frac{2}{9}\mu\xi - \Pi_3.$$ (5.19)

Applying the boundary condition at the front we find that

$$\frac{2}{9}\mu\xi_f = \Pi_3$$ (5.20)

. Integrating directly Eqn. 5.19 we find

$$\frac{K}{\mu}\phi(\xi) = \frac{1}{9}\mu\xi^2 - \Pi_3\xi + c_2.$$ (5.21)

The constant of integration c_2 can be evaluated using the boundary condition at the front $\phi(\xi_f) = 0$ so that

$$\frac{K}{\mu}\phi(\xi) = \frac{1}{9}\mu(\xi^2 - \xi_f^2) - \Pi_3(\xi - \xi_f).$$ (5.22)

The position of the front satisfying the boundary condition is given by

$$\hat{x}_f(\hat{t}) = \frac{\mu}{(aK^2)^{1/3}}\xi_f\hat{t}^{2/3} + \frac{\mu}{aK}.$$ (5.23)

Differentiating with respect to time we find

$$\hat{u}_f = \frac{d\hat{x}_f}{d\hat{t}}$$
$$= \frac{2}{3}\frac{\mu}{(aK^2)^{1/3}}\hat{t}^{-1/3}\tilde{\xi}_f$$

which is the same as if we had used the self-similar solution given by Eqn. 5.18. From the condition that the local slope vanishes at the front, Eqn. 5.20, we find

$$\tilde{\xi}_f = \frac{9}{2\mu}\Pi_3, \tag{5.24}$$

so that the position of the front Eqn. 5.23 is

$$\hat{x}_f(\hat{t}) = \frac{9}{2}\hat{t}^2 + \frac{\mu}{aK}, \tag{5.25}$$

after using Π_3 from Eqn. 5.14. The front increases from the initial value $\frac{\mu}{aK}$ following a parabolic time dependence. The speed of the front is

$$\hat{u}_f = 3\hat{t}, \tag{5.26}$$

linear in the dimensionless time. Using Eqn. 5.20 we can write the solution given by Eqn. 5.22 as

$$\frac{K}{\mu}\phi(\tilde{\xi}) =$$
$$= \frac{1}{9}\mu(\tilde{\xi}^2 - \tilde{\xi}_f^2) - \Pi_3(\tilde{\xi} - \tilde{\xi}_f)$$
$$= \frac{1}{9}\mu(\tilde{\xi}^2 - \tilde{\xi}_f^2) - \frac{2\mu}{9}\tilde{\xi}_f(\tilde{\xi} - \tilde{\xi}_f)$$
$$= \frac{1}{9}\mu(\tilde{\xi}^2 - \tilde{\xi}_f^2 - 2_f + 2\tilde{\xi}_f^2)$$
$$= \frac{1}{9}\mu(\tilde{\xi} - \tilde{\xi}_f)^2,$$

so that we can write

$$\phi(\tilde{\xi}) = \frac{\mu^2}{9K}(\tilde{\xi} - \tilde{\xi}_f)^2$$
$$\psi(\tilde{\xi}) = \frac{2\mu}{3}\tilde{\xi}. \tag{5.27}$$

5.3. Discussion

A self-similar solution of the shallow water equations for the release of a constant volume of granular material has been found by means of dimensional analysis. The height and velocity of the granular fluid are expressed in terms of the dimensionless functions ϕ, ψ given by Eqns. 5.27. In terms of the rescaled height and velocity, Eqns. 5.11, the solutions are

$$\hat{h} = \frac{\mu^2/9K}{(a^2K)^{1/3}}\hat{t}^{-2/3}(\xi - \xi_f)^2$$
$$\hat{u} = \frac{2\mu/3}{(aK^2)^{1/3}}\hat{t}^{-1/3}\xi$$

(5.28)

which become

$$\hat{h} = \left(\frac{\hat{x} - \hat{x}_f}{3\hat{t}}\right)^2$$
$$\hat{u} = \frac{2}{3}\frac{\hat{x}}{\hat{t}}.$$

(5.29)

after substitution of ξ as given by Eqn. 5.12. In terms of the original variables x and t we have

$$h = \frac{\mu^2}{9gK}\left(\frac{x - x_f}{t}\right)^2$$
$$u = \frac{2}{3}\mu\frac{x}{t}.$$

(5.30)

with the front of the granular flow given by

$$x_f(t) = x_0 + \frac{9}{2\mu}gt^2.$$

(5.31)

These solutions are valid in the region $0 \leq x \leq x_f$ and for all times $t > 0$. The height of the granular flow varies with the position parabolically while the velocity of the flow increases linearly with position. It is interesting to observe that the position of the front shows a parabolic dependence on time given by the position

of free fall modulated by the friction coefficient. The speed of the front is

$$u_f = \frac{9}{\mu} gt,$$

which becomes of the order of unity when time $t \sim \mu g^{-1}$ and the position of the front becomes $x_f \sim x_0 + \frac{9}{2}\mu/g$.

The solution found is particular for the following reasons: first, the right hand side of the second of Eqns. 5.15 is not exactly a constant as it depends on the rescaled time. Nevertheless, the solutions found coincide with the self-similar solutions constructed by others [8, 14, 37] using more complex methods. It is possible to remove all time dependence on Eqns. 5.15 using a length scale of the form

$$\xi = xt^{-2},$$

but the resulting equations can not be integrated directly.

The objective of this Chapter was to show how dimensional analysis can lead to self-similar solutions when a mathematical formulation of the problem exists, which we have accomplished with Eqns. 5.27.

CHAPTER 6

EXAMPLE 2. COLLAPSE OF COLUMNS FORMED BY ELONGATED GRAINS

In Chapter 3, based on the experimental evidence presented in Chapter 2, we argued that the phenomenon of the collapse, characterized using the maximum height function (which measures the height of the emplacement as the collapse occurs), has a self-similarity of the first kind on the parameter $d/h_0 \ll 1$. This means that a column comprised of grains with a typical larger (or smaller) size will follow the same scaling laws, as long as the ratio d/h_0 remain small.

A column comprised of larger grains will have a greater initial height h_0, but as long as $d/h_0 \ll 1$, the same scaling laws will hold and the maximum height function will continue to have the property of self-similarity of the first kind with respect to this parameter. Under this condition, this implies that the properties of the collapse are independent of the typical size of the grains used.

But, what about the shape of the grains? In the list of possible relevant parameters influencing the phenomenon, we did not consider explicitly the shape of the grains. In some of the experiments described in Chapter 2, collapses were performed with columns made of grains of different shapes, but as this effect was not the

main objective of their investigations, no conclusive evidence of the dependence on the shape of the grains was provided. Under certain constraints, as an effect of the elongation, grains tend to self-organize into a preferred direction along which they align during motion [6, 10, 45], changing the flow properties and reaching steady states that reflect this alignment preference.

In the granular column collapse, until [44] and [42], no systematic study of the dependence on the shape, in particular on the elongation of the grains, on the collapse of granular columns was reported. These works found that the scaling laws of the form $\sim a^\beta$ still hold for collapses of columns made with elongated grains and is the topic of this Chapter.

The contents of this Chapter are presented verbatim as it appeared published in Physical Review E under the title "Computer simulations of the collapse of columns formed by elongated grains" by Horacio Tapia-McClung and Roberto Zenit (`http://pre.aps.org/abstract/PRE/v85/i6/e061304`). The work leading to this article is part of the study of the dependence in the collapses of granular columns on the relevant parameters, in particular in this case, the shape of the grains, focusing on elongated grains.

6.1.   Results

Columns are constructed by randomly placing a total number $N_t = 2000$ of grains of type N_k, where k is the number of circular grains used to make an elongated one, between two walls whose half separation determines the initial length, x_0 of the column. The simulation parameters used here correspond to glass particles of diameter $\bar{d} = 0.3mm$ with a 10 % size distribution, except for the friction coefficient between grains, which was chosen equal to $\mu = 0.5$ to directly compare with the results reported in [46].

Once the grains have settled under gravity and reached an equilibrium state, the maximum height of the particles, h_0, is measured and the value of the corresponding parameter a is obtained for the column. In this way we prepare columns with initial aspect ratio values a in the interval $[0.3, 15]$ for elongated grains of types: N_1 (circular grains), N_3, and N_5; only a few cases where run for N_8. At $t = 0$ the walls are removed instantaneously, releasing the grains and initiating the co-

llapse. When the grains come to a stop, the final maximum height and extension of the deposit are measured. No systematic study of the dependence of the collapse on the preparation of the columns was performed. During the collapse, an energy balance is performed as described in Chapter 4.

The main result is that the final distances that characterize the collapse scale with the initial aspect ratio, a, similar to columns made of circular grains. For all types of grains used, a monotonic increase (decrease) of the final run-out (height) with a is observed. The scaling exponent seems to depend weakly on the elongation of the grains.

Energy calculations like those shown in Figure 3 of the article, indicate that the final properties of the deposits can be understood in terms of the energy conversion of the system as the collapse occurs: columns with similar values of initial aspect ratio a transform the initial potential energy in such a way that the final properties of the deposit are similar, irrespective of the type of grains used, as long as they are not extremely aspherical [12, 15]. The use of the the available energy for spreading does not depend on the type of grain used but does depend on the value of a, as with circular grain columns[39].

The time evolution of the inertial number I shows a quick decrease for short times $\tau < 1$. Then I reaches a steady value close to 0.02 regardless of the grain type and we conclude that the shape of the grains does not modify the effective friction in a significant manner. Therefore, it is not surprising that the run-out is similar for all grain types.

6.2. Discussion

The results presented in this work show that the collapse does not depend on the type of grain, in particular, on the elongation of the grain. We can therefore use this evidence to assume that the phenomenon of the collapse has a self-similarity of the first kind on a dimensionless parameter involving the shape of the grains, similar to d/h_0. Further the use of the quantity similar to the inertial number provides a tool to characterize the flow and understand the effective friction of the flow in terms of the initial aspect ratio and the elongation of the grains.

CHAPTER 7

EXAMPLE 3. COLLAPSES OF COLUMNS IN DIFFERENT GRAVITIES

From the scaling relations obtained in Chapter 3 using dimensional analysis, time is scaled according to

$$\tau = \frac{t}{(h_0/g)^{1/2}}, \tag{7.1}$$

where h_0 is the initial height of the column and g the gravitational acceleration. The meaning of this scaling can be easily understood if we consider a single grain falling from an initial height h_0 under the constant acceleration g. In this situation, the well known free falling law gives the height of the grain as a function of time

$$h(t) = h_0 - \frac{1}{2}gt^2.$$

If we perform the variable change

$$t \rightarrow \left(\frac{2h_0}{g}\right)^{1/2} \tau,$$

this expression becomes

$$h = \tag{7.2}$$

$$= h_0 - \frac{1}{2}gt^2 \tag{7.3}$$

$$= h_0 - \frac{1}{2}g\left[\left(\frac{2h_0}{g}\right)^{1/2}\tau\right]^2 \tag{7.4}$$

$$= h_0 - \frac{1}{2}g\left(\frac{2h_0}{g}\right)\tau^2 \tag{7.5}$$

$$= h_0(1 - \tau^2) \tag{7.6}$$

so that scaling the grain's height h with the initial height at which it is dropped h_0 results in

$$h^* = (1 - \tau^2), \tag{7.7}$$

with $h^* = h/h_0$. In other words, the dimensionless height of the grain is independent of the initial height *and* on the value of gravity. This means that if the grain is left to fall from an initial height h_0 on Earth or on Mars, the vertical position of the grain is described by the scaling law $1 - \tau^2$, as long as time is measured as $\tau = t/(h_0/g)^{1/2}$, i.e. the free fall of a grain "looks"the same, in the scaled variables h^*, τ on Earth or on Mars.

This chapter explores the question naturally arising from this trivial observation: will a granular column, under the same nominal conditions, collapse similarly on Earth or on Mars? The chapter is presented verbatim as it has been submitted for consideration to be published at the specialized journal "Earth and Planetary Science Letters". Currently the article is in review.

7.1. Results

Varying the gravitational acceleration it is found that the scaling

$$h_\infty/h_0 \sim a^\beta$$

is preserved. Further evidence that the scaling exponent does not depend on the inter-granular friction is provided. When the evolution of the dimensionless height

for similar initial aspect ratio columns is plotted as a function of the gravity dependent characteristic time $\tau = \sqrt{2h_0/g}$ the curves are very close to each other, irrespective of the friction between grains and the value of g. We have also found that the inertial number for all cases lies in the dense flow regime, with high(low) aspect ratio columns having smaller(larger) final values of this quantity. We found that for a given gravity, the inertial number is a decreasing function of the initial aspect ratio.

As the value of gravity is lower, the grains appear to be on a fluidized state during the beginning of the collapse, similar to an observed experimental effect [36]. Since vertical accelerations due to gravity are very low, the grains that collapse at low gravities show less contacts and appear fluidized in a natural way, thus dissipating less energy by frictional contacts. On the other extreme, grains of columns collapsing at large gravities have greater vertical accelerations and tend to compact and present enduring contacts, dissipating energy much faster.

The inertial number I, on which the effective friction of a granular flow depends, has large values for columns collapsing at low gravities, thus fewer contacts between grains occur during the flow. In these cases, according to the μ-rheology, there is a larger effective friction which balances with the lack of dissipation by frictional contacts and making the final height be similar to that of deposits of columns collapsing at higher gravities, where the value of the inertial number is lower and energy is dissipated by enduring friction contacts.

If the initial aspect ratio of the column is large and the collapse occurs under a low gravitational acceleration, a fluidized state develops increasing the pore pressure that eventually diffuses. This initial fluidization reduces the effective friction of the system, due to fewer contacts, leaving the grains enough energy that is dissipated later during the flow, resulting in final distances that are similar to the dry experiments performed on Earth. We have found that the scaling $\sim a^\beta$ is preserved and that the influence of the grains coefficient of friction is weak on the scaling exponent β.

7.2.   Discussion

The results of this study evidence the independence of the collapses on the value of the local gravitational acceleration and provide further indication that the friction between grains weakly affects the collapses. For our purposes, these results confirm that the maximum height of the collapse adheres to the self-similarity assumptions discussed in Chapter 3 and so that the observed scaling laws can indeed be recovered using these ideas.

CHAPTER 8

GENERAL CONCLUSIONS

8.1.   Discussion of results

The collapse of a granular column is a very simple table-top experiment that can be performed almost anywhere. Due to its simplicity it has been explored thoroughly in different configurations and using different materials since the first experiments were reported almost a decade ago. Even today the experiment is used as a paradigm and test case for understanding flows of granular material that occur naturally on Earth and other planets.

A bibliographic search of the problem in specialized journals shows that the problem is far from being outdated, that new discoveries are still being found on this system and it is being used as a comparison test for studying events that are difficult to reproduce at the laboratory scale. Although it has been widely studied, the scaling relations found for the final properties are still not yet well understood. Since there is no theoretical framework that describes a granular flow in full, there is no way to obtain these relations from first principles.

In this thesis we have proposed an approach that explicitly considers the relevant physical parameters to the problem by studying the influence they have using numerical simulations. In Chapter 3 we showed that the parameters that influen-

ce the maximum height function are the dimensionless time, the effective friction and the initial aspect ratio of the column. The effective friction, a property of the flow, can be described by means of the so called μ-rheology [13] in terms of a single dimensionless number, the inertial number I. By using dimensional analysis, the evolution of the maximum height of the emplacement is expressed in terms of dimensionless parameters and their influence on the maximum height of the collapse is explored numerically by means of simulations using a Discrete Element Method described in Chapter 4.

As an example of the application of dimensional analysis, a self-similar solution is constructed analytically from a simple mathematical model in Chapter 5. The self-similar solution found coincides with solutions for the release of a constant volume of fluid constructed by different methods [8, 37]. This self-similar solution describes the height and velocity of the granular fluid at the intermediate state when certain details of the initial conditions cease to be relevant to the flow [4, 5], when some parameters remain small (or large) thus not influencing the system; in this case, the initial width of the column and thus the initial aspect ratio parameter.

Clearly the system is an idealized simplification of the model, but is serves its purpose as a good example for constructing self-similar solutions, and it could be used, in principle, to study the more realistic case of a column with a larger initial aspect ratio, as long as the assumptions leading to the system are still valid.

We postulate that the effective friction during the collapse changes as the elongation of the grains used to form the columns increases, and so the final height and runout distance of the deposits depend on this parameter. To explore this dependence we performed numerical simulations of the collapse of granular columns made of elongated grains, and present the results of this work in Chapter 6.

It was found, as in the experimental work of [44], that the power law scaling is preserved when columns made of elongated grains collapse [42, 44]. This can be interpreted as the maximum height having a self-similarity of the first kind on a parameter relating to the elongation of the grains. This work also introduces a dimensionless quantity similar to the inertial number I that characterizes the flow in terms of its values. It was found that for elongated grains the shape does not modify the effective friction in a significant way. These results have been published as an article in the specialized journal Physics Review E.

The next relevant parameter is the dimensionless time. This is normalized using the value of the local gravity, thus any change on this acceleration should be reflected in a change of the maximum height of the emplacements. We have performed numerical simulations of columns comprised of grains with different friction properties in different gravities, and found that the scaling of final height with the initial aspect ratio is preserved, and that for short dimensionless times the collapses follow the free fall scaling law very closely.

This means notably, that at the macroscopic level the emplacements occur similarly on Earth or on Mars. At the grain scale differences arise, specially in low gravities: due to the small vertical accelerations grains are less in touch during the first stages of the collapse, effectively causing a natural fluidization that reduces the effective friction, which is, notwithstanding, increased again when the grains are in contact in the second stage of the collapse. This effect is more pronounced for columns with large initial aspect ratios collapsing in low gravities. These results have been submitted as an article to the journal Earth and Planetary Science and is currently under revision.

8.2.   Final remarks

The results obtained in this research consistently show that the scaling of the final distances characteristic of emplacements formed by the collapse of granular columns- columns made of elongated grains, and columns collapsing on different gravities (including Earth)- have final properties that scale as a power law of the initial aspect ratio parameter. This suggests something like a "universality" of this scaling law. Dimensional analysis shows that the dependence of quantities like the maximum height of the emplacement depend, among others, on this crucial parameter.

The presence of such a scaling law indicates that the collapse is self-similar. As discussed in Chapter 3, this implies that different columns that have the same initial aspect ratio, regardless of the particular characteristics, like the grains they are made of, if they are collapsing under different substrates, even if they have different initial widths and heights, will collapse such that the final distances scale in a similar way.

This observation, supported by the experimental evidence is the starting point to apply the formalism developed by [4, 5], known as self-similarity of the first and second kind to obtain, mathematically, the power law scaling. By postulating that the maximum height of the deposits, and therefore the final height, have a self similarity of the second kind on the initial aspect ratio parameter, the experimentally observed and confirmed power law scaling for this quantity is recovered.

After that, numerical simulations are performed, where values of the parameters are varied to explore both the validity of this scaling law and the value of the scaling exponents, for which neither dimensional analysis nor the self-similarity formalism provide information.

8.3.   Future work

In this work, we focus on the power law scaling with the initial aspect ratio parameter of the maximum height of the deposits. Clearly this does not give a complete description of the phenomenon nor is it characterized in full. Most research focuses on the final runout largely because for hazard assessments, this quantity seems to be more relevant that the final height. Future work is required to study the evolution of the front of the deposits as the collapse occurs.

No results on the velocity profiles of the grains during the collapse have been presented, which are fundamental to understand the flow. Few visual comparisons have been performed during the course of this research of the speed of the grains as they collapse under different gravities, finding that, when scaled appropriately with the value of the local gravity, the column falls at the same speed. No systematic research has been done in this direction, but the feeling is that by scaling the velocities of the grains, a similar result as that with the maximum height can be obtained.

A mathematical expression for the profile of the columns, $h(x, t)$ that contained all the information about the emplacements is a first step to describe the collapse of a granular column. Such an expression is no doubt, difficult to obtain, and we have provided some initial insight towards the properties this function must have.

It is rather surprising that the power law scaling is obtained under so many different circumstances. Of course, final runouts from natural events are not as ideal

as controlled experiments or numerical simulations, and in general do not follow these scaling laws so well, therefore, a system with the characteristics of the granular collapse which deviate from these scaling laws is desired. A column collapse comprised of polydisperse grains would be a candidate, and represents the next natural step to study the problem.

.1.   **Appendix**

In the next pages we present the journal article and manuscript documents containing the results of collapses of columns made of elongated grains (Chapter 6) and of collapses of columns under different gravities (Chapter 7).

The first document is shown as it appear published in the specialized journal Physical Review E under the title "Computer simulations of the collapse of columns formed by elongated grains" which can be found in the following url link: `http://pre.aps.org/abstract/PRE/v85/i6/e061304`.

The second document is the manuscript sent for consideration to the journal Earth and Planetary Science Letters, and for which we are waiting response at the time of this writing.

Computer simulations of the collapse of columns formed by elongated grains

Horacio Tapia-McClung[*] and Roberto Zenit

Instituto de Investigaciones en Materiales, Universidad Nacional Autónoma de México, Apdo. Postal 70-360, Ciudad Universitaria, Coyoacán D.F. 04510, México

A numerical investigation of the collapse of granular columns has been conducted. In particular, we address the effect of the grain shape on the properties of the collapse. We show that the final runout and height of the deposits scale as a power law of the initial aspect ratio of the column, a, independently of the elongation of the grains used. We describe this process in terms of an energy balance, and construct an "inertial number" that can be used to describe the flow in terms of a recently proposed granular rheology. We argue that an effective friction that results from this dimensionless quantity explains why the shape of the grains is irrelevant for the final properties of the collapse.

I. INTRODUCTION

The dynamic behavior of granular materials is fundamental in many natural and industrial phenomena where the flow and accumulation of particles is of central concern. Many anthropogenic and natural processes, like road construction and landslides, involve a granular phase which displays a behavior that differs from that of ordinary fluids. Despite their ubiquity, the understanding of granular materials is still a developing subject that requires the collaboration of many fields of knowledge. Much of what is known of granular matter is the result of recent experimental studies and numerical simulations that complement the empirical knowledge obtained by many years of experience and use of these materials.

A simple experiment that has received attention in recent years is that of the sudden collapse of vertical granular columns, where the flow is driven only by gravity. The original experiments [1,2] released granular materials from a cylindrical container into a flat horizontal surface and studied the flow and properties of the final deposits. In a different setup, the cylindrical column was replaced by a rectangular step [3–5]. In both cases, it was found that the final state of the deposits, characterized by the total distance traveled in the radial (or horizontal) direction and the final height of the deposited mass, scale with the column aspect ratio [1–7]. The aspect ratio, a, is defined as the ratio of the initial height h_0 to the initial radius r_0 (or the initial horizontal extension x_0) of the column: $a = h_0/x_0$.

Numerical studies that take into account the discrete nature of the system have been able to reproduce experimental observations using different numerical schemes [3,6,7]. So far, these simulations have considered only spherical particles or disks to model grains. Real granular materials involve a large collection of particles with different properties, including different shapes and sizes, that can have an effect on the collective behavior of the grains. It is interesting to note that the results of Refs. [2,4] suggest that the scaling properties of the collapsed columns do not depend strongly on the shape of the grains used. In most experiments, a single type of elongated

grains were used having similar friction properties as the round particles. The same scaling law was observed. Because these works were not explicitly looking for the effect of particle shape on the final properties of the collapses, this question remained unanswered. Recently, a systematic experimental study has addressed this issue [8].

Whereas the effect of the shape of the grains has not been fully explored in the column collapse problem, it has been addressed in other configurations. Elongated granular materials, like rods, show a phase transition from a disordered to an ordered state on a preferential direction exclusively as a result of the elongation of the grains [9,10]. Rods and elongated grains have a larger surface area on which friction acts modifying the dynamics observed on circular grains. While circular grains can have high packing fraction values, elongated particles tend to leave many voids, decreasing the packing fraction, which will also cause different dynamics when the grains flow [8].

In this paper we present results of the scaling properties of the final deposits of the collapse of 2D granular columns made of grains with different elongations obtained with numerical simulations. Individual circular grains are modeled as soft disks that interact under prescribed elastic and viscous contact forces in the normal and tangential directions, while elongated grains are created by "gluing" two or more circular grains and constraining them to a linear geometry. Elongated grains made of k circular grains are denoted by N_k; for example, N_1 refers to circular grains, N_2 to elongated grains made of two circular grains, and so on.

II. NUMERICAL SCHEME AND PARAMETERS

Numerical simulations of the collapse of granular columns were performed using a discrete element method similar to that used in Ref. [7], as an idealization of the experimental studies of Refs. [1,2].

Details of the numerical algorithm, which integrates Newton's equations of motion for each grain of the system, can be found in Ref. [7]. It is based on a second-order velocity-explicit Verlet method [11,12] in which grains interact only at contact by prescribed elastic and viscous forces in the normal and tangential direction. The friction between grains is modeled using a Coulomb type sliding friction determined by the

[*]horaciotmc@iim.unam.mx

value of the friction coefficient μ. The only external force on the grains is gravity. To create an elongated grain an extra force, determined by evaluating the Lagrange multipliers, is necessary to maintain k circular grains constrained to a linear geometry at all times. This method is implemented and described in full detail in Ref. [12].

Columns are constructed by randomly placing a total number $N_t = 2000$ of grains of type N_k between two walls whose half separation determines the initial length, x_0 of the column. The simulation parameters used here correspond to glass particles of diameter $\bar{d} = 0.3$ mm with a 10% size distribution, except for the friction coefficient between grains, which was chosen equal to $\mu = 0.5$ to directly compare with the results reported in Ref. [7]. Once the grains have settled under gravity and reached an equilibrium state, the maximum height of the particles, h_0, is measured and the value of the corresponding parameter a is obtained for the column. In this way we prepare columns with initial aspect ratio values a in the interval $[0.3, 15]$ for elongated grains of types: N_1 (circular grains), N_3, and N_5; only a few cases where run for N_8. At $t = 0$ the walls are removed instantaneously, releasing the grains and initiating the collapse. When the grains come to a stop, the final maximum height and extension of the deposit are measured.

We did not perform a systematic study of the dependence of the collapse on the preparation of the columns. Based on previous results [13], it is expected that the initial packing fraction will have an influence on the collapse process. We performed a few test simulations of columns prepared by initially placing elongated grains parallel or transverse to the horizontal surface (on which the collapse occurs) with the most clear difference being that the column may not collapse (results not shown). Clearly, a more in depth study would be needed to assess this issue for the particular case of elongated grains.

III. RESULTS

A. Final runout and height

For each column the normalized final runout distance x_∞, and final height h_∞, measured at the end of the collapse are shown in Fig. 1 as a function of the column aspect ratio a. The results are consistent with the previously observed monotonic increase (decrease) of $x_\infty(h_\infty)$ as a increases (decreases). The general features of the collapse process are captured by our simulations; a good agreement with previous results [6,7] is observed. Surprisingly, the data on Fig. 1 show similar scaling features for all types of grains, with the circular grains (type N_1, red solid circles) having the largest final runout values and the N_5 type grains (black diamonds) having the lower runout values. The final runout measurements for grains of type N_3 (blue squares) and N_8 (green triangles) lie in between these two and remarkably close to each other. A similar behavior can be observed for the final height of the deposits, shown as the corresponding open symbols in the figure. We can, in part, attribute the small differences in the results for different grains to the uncertainty that arises from considering a "small" number of particles.

The results of Fig. 1 allow us to write a scaling law for the final runout distance with the column aspect ratio of
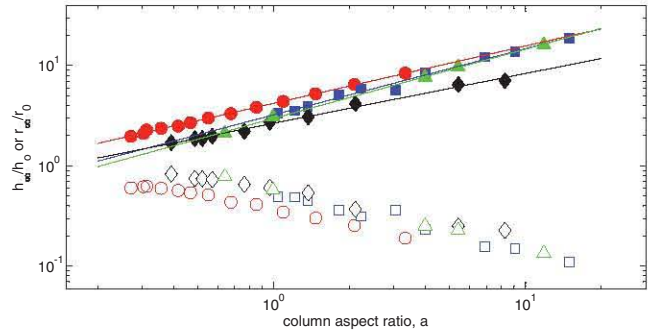

FIG. 1. (Color online) Final runout (filled symbols) and height (empty symbols) as a function of the column's initial aspect ratio a for columns made of long grains of type N_1 (circle), N_3 (square), N_5 (diamond), and N_8 (triangle). The dashed lines correspond to the fit that gives the scaling exponent of Table I.

the form

$$\frac{r_\infty}{r_0} \sim a^{p_k} \tag{1}$$

and a similar expression for the final height h_∞. By performing a fit to the data of Fig. 1, we obtain the values shown in Table I for the exponent p_k. Despite the small differences for each case, these exponents are within the same range as those found in the experiments [1–5] and numerical simulations [6,7] for the collapses of columns for circular grains, reinforcing the hypothesis that the final runout distance of the collapse of granular columns scale similarly and independently of the types of grains used.

The final height of the columns, h_∞, shown in Fig. 1 as open symbols, indicate that columns made of larger grains collapse into deposits that are slightly taller than columns made of shorter grains. In accordance with Ref. [8] the collapse follows the same scaling law with the column initial aspect ratio.

B. Evolution of collapse

There are known differences in the dynamics of round and elongated particles [9,10]. To us, it is perplexing to observe that such an effect has little influence on the final properties of the deposits that results from column collapses. To further investigate this issue, we now turn our attention to the process that takes place from the initial column state to the final deposit. Figure 2 shows snapshots of the column collapse process at different instants for a particular column aspect ratio ($a \approx 4$). We compare three cases for grains of different lengths ($N_1, N_3,$ and N_8) at dimensionless times $\tau \approx 0.0, 0.3, 0.6, 1.5,$ and 3.0 where $\tau = t/\sqrt{2h_0/g}$.

TABLE I. Scaling exponents of the final runout distance as given in expression (1). The values correspond to the slopes of the straight lines shown in Fig. 1.

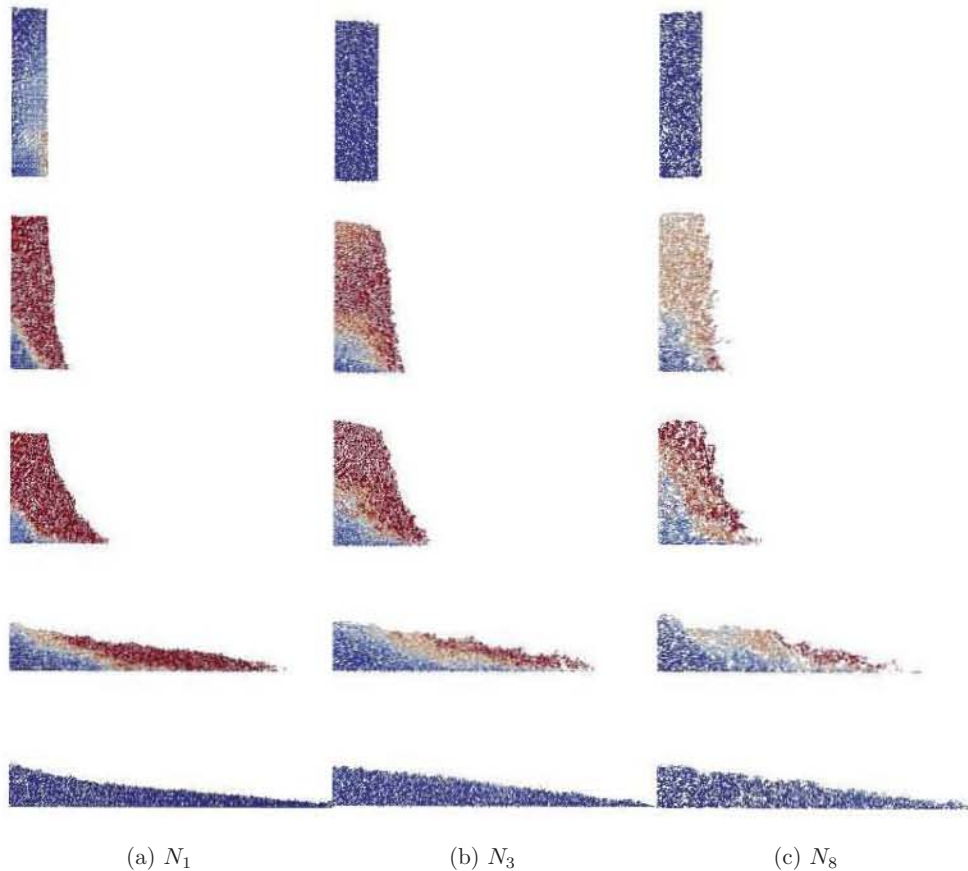| Grain type	p_k
N_1	0.57 ± 0.02
N_3	0.66 ± 0.07
N_5	0.50 ± 0.05
N_8	0.69 ± 0.03

(a) N_1 (b) N_3 (c) N_8

FIG. 2. (Color online) Snapshots of the column collapse process for a column aspect ratio $a \approx 4$. Each row shows a snapshot taken at the dimensionless time $\tau \approx 0.0, 0.3, 0.6, 1.5$, and 3.0 (from top to bottom) as indicated in Fig. 3. Light gray (blue online) shading to dark gray (red online) shading colors indicate increasing grain speed. Note that only the right side of the collapses are shown as they are very symmetric.

For the three columns shown, at all times the collapse process looks similar. During the collapse, the height and extension of the columns are indistinguishable from the figure. Regions of static and moving grains that change in shape as the collapse occurs can be observed. At $\tau \approx 0.3$ a nearly triangular region of static grains of type N_1 can be observed at the bottom of the column. For longer grains this static region appears less regular in shape and it covers a larger area. We can also notice that at this instant of the collapse there is a larger portion of circular grains that have acquired kinetic energy (color indicates speed), whereas for longer grains (type N_8) fewer grains appear to have a lower energy, as can be seen by the difference in color.

At a later time $\tau \approx 0.6$, a surface of flowing grains develops in all three columns, but the region of static grains has increased in size, most noticeable for longer grains. The height of the static region is about half the maximum height of the column at that instant, whereas for circular grains the static region is much smaller for the same time. Longer grains have less mobility as they compact due to their shape. At this instant, which coincides with the time for which the maximum kinetic energy is reached (see below), about 2/3 of the circular grains are participating in the flow while for longer grains only half of the grains are moving. Until this time, the shape of

the collapsed columns still looks similar for all grain shapes and, except for the aspects we just discussed, no significant differences can be observed.

At $\tau \approx 1.5$ the collapses are near the end of the avalanche phase and moving grains flow over a bed of static grains below. During this period of time grains slow down, dissipating energy mostly by friction. Notice that the region of static grains has increased in extension in all three cases but we can still observe that more circular grains participate in the flow. The deposit of larger grains has more irregularities on the surface than that for circular grains and a smaller portion of grains are moving. When the grains have dissipated all their energy, the final deposits have a different shape due to the irregularity created by the longer grains: The column made of circular grains ends up with a deposited mass that has a well-defined maximum tip, while the long grain deposits show a more rounded surface profile. On closer inspection, the surface for grains of type N_8 reveal a more irregular surface than for the other columns. Nevertheless, the overall final extent of the deposits is similar for all cases, as shown in Fig. 1.

Some of the dynamic differences among the collapses for different grains can be quantified if we consider an energy balance. Following Ref. [7], we plot the dimensionless mean potential and kinetic energy of the grains (normalized by the
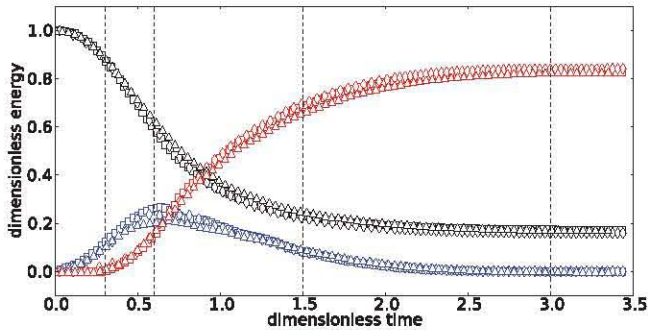
FIG. 3. (Color online) Dimensionless energies as a function of time for columns with initial aspect ratio of $a \approx 4$. Symbols are the same as in Fig. 1 for grains of type N_3 (square), N_5 (diamond), and N_8 (triangle). The vertical lines indicate the times at which the snapshots of Fig. 2 where taken. Black curves show E_p^*, blue E_k^*, and red E_{dis}^*.

initial total energy of the column), E_p^* and E_k^*, together with the cumulative dissipated energy during the collapse,

$$E_{\mathrm{dis}}^* = 1 - E_p^* - E_k^*.$$

Figure 3 shows the energy balance for the columns shown in Fig. 2. The vertical lines on this plot indicate the instants of time at which the snapshots of Fig. 2 where taken. The kinetic energy of the grains increases monotonically to a maximum value that depends on the type of grains used; the shorter grains gain more kinetic energy. One can expect longer grains to accelerate at a slower rate since their surface area is greater; friction forces between these grains act through a longer distance. After this acceleration phase, grains decelerate and E_k^* decreases monotonically, again, at a slower rate for longer grains. Finally, by the end of the collapse, the kinetic energy E_k^* of all columns reaches a zero asymptotic value when they come to rest after dissipating their energy; columns made of shorter grains dissipate energy at a faster rate than columns made of longer grains, as can be seen from the red curves for the cumulative dissipated energy E_{dis}^*. The potential energy E_p^* of the grains, which can be related to the maximum height of the column, also behaves similarly for all columns: It decreases monotonically as time progresses until it reaches a finite value. For the columns made with longer grains, the rate at which the grains convert potential energy to kinetic energy is slower than that for circular grains. The intermediate case of N_3 type grains falls in between. Surprisingly, all three columns reach nearly the same final value of E_p^*, supporting the observation that the final properties of the collapse scale similarly with the parameter a and do not depend on the type of grain used [2,4,8].

IV. DISCUSSION AND CONCLUSIONS

Numerical simulations of the collapse of 2D columns capture the main features of laboratory experiments very well. For columns made with grains of different elongations, we have found that the final distances that characterize the collapse scale with the initial aspect ratio, a, similarly to columns made of circular grains. For all types of grains used, a monotonical increase (decrease) of the final runout (height) with a is observed. The scaling exponent seems to depend weakly on

the elongation of the grains. Energy calculations like those shown in Fig. 3 indicate that the final properties of the deposits can be understood in terms of the energy conversion of the system as the collapse occurs: Columns with similar values of initial aspect ratio a transform the initial potential energy in such a way that the final properties of the deposit are similar, irrespective of the type of grains used.

Recently, significant advances have been reached in the rheological description of granular flow [14]. A single dimensionless number, the inertial number I, has been used to describe flow properties, in particular for the transient flow in the column collapse problem [15,16]. Since this approach has proven quite successful we have used some of these ideas to explain our results. We construct a quantity equivalent to the inertial number, which is the ratio of two characteristic times of the flow during the columns collapse.

The use of the the available energy for spreading does not depend on the type of grain used but does depend on the value of a, as with circular grain columns [6]. In the energy plots of Fig. 3 we notice that the conversion of the available energy from potential to kinetic is very similar for all grains. When the deposit experiences horizontal deformation (not during the initial phase of the collapse) the rate of deformation can be approximated by

$$\dot{\gamma} \approx \frac{x(t) - x_0}{t} \frac{1}{h_0 - h(t)}.$$

On the other hand, we can construct a characteristic time from the pressure of the whole column at the base $P = \frac{Mg}{x - x_0}$, where M is the total mass of the column. Considering an effective diameter $d_{\mathrm{eff}} = \bar{d}\sqrt{k}$ (k being the number of circular grains of mean diameter $\bar{d}$ that make an elongated grain of type N_k) we can construct a pressure time scale as

$$T_P = d_{\mathrm{eff}} \frac{(x - x_0)^{1/2}}{\sqrt{c_0 A g}},$$

where $c_0 A$ is the initial area occupied by the grains in the column. Comparing the pressure time scale with the effective shear rate, the inertial number can be written as

$$I = \frac{d_{\mathrm{eff}}(x - x_0)^{3/2}}{h - h_0} \frac{1}{t\sqrt{c_0 A g}}. \tag{2}$$

In agreement with what has been discussed in Ref. [14], large values of I indicate that the pressure of the material
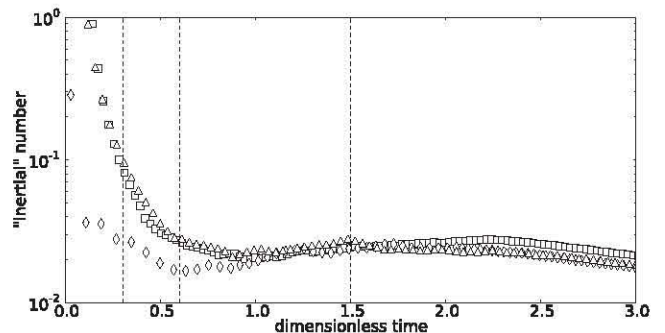

FIG. 4. Time evolution of the inertial number I from Eq. (2) during collapse for the columns of Fig. 2. Symbols and vertical lines are the same as in Fig. 3.

above dominates over horizontal deformation of the deposit, as expected for short times. As times advances, I decreases as the shear deformation becomes important

Figure 4 shows the time evolution of I for the data shown in Fig. 3. We see that I quickly decreases for $\tau < 1$. Then I reaches a value close to 0.02 for all cases, regardless of the grain type. Following Ref. [14] we can argue that the effective friction is approximately the same for all grain types considered: The shape of the grains does not modify the effective friction in a significant manner. Therefore, it is not surprising that the runout is similar for all grain types.

In summary, our numerical results are in close agreement with previously reported results for the column collapse problem [2,4,8]. We have shown that some differences can be observed during the collapse for different grain length; however, such differences do not affect the global friction coefficient in a significant manner. To us it remains a challenge to understand why the grain shape does not influence the global behavior of the collapse.

[1] E. Lajeunesse, Mangeney A. Castelnau, and J. P. Vilotte, Phys. Fluids **16**, 2371 (2004).

[2] G. Lube, H. E. Huppert, R. S. J. Sparks, and M. A. Hallworth, J. Fluid Mech. **508**, 175 (2004).

[3] N. J. Balmforth and R. R. Kerswell, J. Fluid Mech. **538**, 399 (2005).

[4] G. Lube, H. E. Huppert, R. S. J. Sparks, and A. Freundt, Phys. Rev. E **72**, 041301 (2005).

[5] L. Lacaze, J. C. Phillips, and R. R. Kerswell, Phys. Fluids **20**, 063302 (2008).

[6] L. Staron and E. J. Hinch, J. Fluid Mech. **545**, 1 (2005).

[7] R. Zenit, Phys. Fluids **17**, 031703 (2005).

[8] M. Trepanier and S. V. Franklin, Phys. Rev. E **82**, 011308 (2010).

[9] D. L. Blair, T. Neicu, and A. Kudrolli, Phys. Rev. E **67**, 031303 (2003).

[10] D. Volfson, A. Kudrolli, and Lev S. Tsimring, Phys. Rev. E **70**, 051312 (2004).

[11] M. P. Allen and D. J. Tildesley, *Computer Simulation of Liquids* (Oxford University Press, Oxford, 1989).

[12] H. Tapia-McClung and N. Grønbech-Jensen, J. Polym. Sci., Part B: Polym. Phys. **43**, 911 (2005).

[13] A. Daerr and S. Douady, Europhys. Lett. **47**, 324 (1999).

[14] GDR MiDi, Eur. Phys. J. E **14**, 341 (2004).

[15] L. Lacaze and R. R. Kerswell, Phys. Rev. Lett. **102**, 108305 (2009).

[16] P.-Y. Lagrée, L. Staron, and S. Popinet, J. Fluid Mech. **686**, 378 (2011).

Computer simulations of the collapse of granular columns in different gravities

Horacio Tapia-McClung*, Roberto Zenit*

Instituto de Investigaciones en Materiales,
Universidad Nacional Autónoma de México,
Apdo. Postal 70-360, Ciudad Universitaria,
Coyoacán D.F. 04510, México

Abstract

We present a numerical study of the collapse of two dimensional granular columns under different gravitational accelerations. We find that the final properties of the emplacements are not strongly affected by the value of the gravitational acceleration and that the scaling law $\sim a^\beta$ is preserved. An energy balance shows differences for high aspect ratio columns collapsing in low gravities which results from a fluidization of the column induced by the grain motion.

Keywords: Granular Column Collapse, Discrete Element, gravity, scaling law

1. Introduction

Dense gravity-driven granular flows play an important role in shaping the surface of the Earth and other planets. These complex processes involving solid particles interacting with an interstitial fluid (like air or water) are abundant in nature, and represent a natural hazard threatening many anthropogenic activities. Similar events have been observed in extraterrestrial planets like the Valles Marineris (VM) landslides on Mars ([13, 16, 10]); they represent a good comparison and a test to the knowledge acquired from experiments and numerical simulations done under terrestrial conditions.

Many theoretical and experimental studies have tried to determine the relevant parameters that influence this events in order to characterize these flows and

---

describe the phenomena occurring in Nature. Laboratory experiments of the collapse of granular columns under controlled conditions ([8, 12, 9, 11, 6, 1]) have shed some light into the physics of these flows having established well defined unique scaling laws of the final distances that primarily depend on the initial geometry of the columns. Dense granular flows in natural events are more complex phenomena involving many different interacting components and usually have much less energy dissipation than the controlled experiments ([13, 16]). For example, studies of the VM landslides (Mars) ([13]) have shown some disagreement on the final run-out distances with experiments and theoretical models, which suggests that some mechanisms result in significantly smaller energy dissipation than that for typical dry flows ([13, 16]). Similar natural phenomena on Earth also show signatures of a significantly smaller effective friction resulting in larger run-out distances that in the dry flow cases ([16]).

Recently ([16]), an experimental study of the collapse of a column which is initially fluidized has shown that the scaling laws of the form λa^n are more general than those observed for dry grains only. The initial fluidization of the grains increases the interstitial porosity considerably reducing the inter-granular friction. As the column collapses the pore pressure diffuses with an increase on the internal friction that still remains below that of a dry (non-fluidized) equivalent. This initial fluidization and decrease on the internal friction does not change the scaling laws and only changes the value of the coefficient λ compared to dry dense flows, but show no significant change in the value of the scaling exponents ([16]). This work also reveals that the exponent n is independent of the mean friction of the flow. Comparison of experimental results with data of the VM landslides on Mars ([13, 16]) suggests a lower effective friction as a physical mechanism contributing to low energy dissipation during the emplacement of these extraterrestrial events and thus longer run-out distances. This conclusion is reached in the context of the thin layer approach (or the Saint-Venant equations) together with a Coulomb type friction law ([13, 16]), a simple model that has successfully reproduced experimental results for a limited range of the parameters ([15]).

Numerical experiments, even with such minimal models as the one used by ([15]), are in very good agreement with experimental results on dry flows ([8, 12, 9, 11]) and are capable to reproduce the scaling laws observed in the experiments. While some discrete element methods tend to overestimate the run-out distance compared to the experiments ([19, 17]), others successfully reproduce experimental data ([6]). Overall, they have been used as a powerful tool to investigate this kind of problems. The nature of these methods allows some

effects that escape the continuous models and that may be relevant to understand the geological observations. In particular we are interested in the effects of gravity at the particle scale and how this reflects in the final properties of the emplacements. Arguably, the behavior of dense granular flows is strongly dependent of frictional forces. As the granular mass flows, the grains remain in enduring contacts exerting frictional forces on each other. In the column collapse problem, the force which maintains the grains in contact is their own weight which, naturally, depends on the value of the local gravity. Hence, we wonder if one can expect the same granular rheology if the gravitational acceleration is changed. Under the same nominal conditions (same granular mass and initial conditions), would an avalanche run out farther, shorter or the same on Earth or Mars? Using DEM modeling we aim to answer this question and to that matter we perform numerical simulations of the collapse of dry granular columns and vary the inter-granular friction and the values of the gravitational acceleration.

We briefly describe the numerical model used and the parameters controlled and varied in the numerical experiments in section 2. Then a short discussion on the dimensional analysis of the problem is presented in section 3. In section 4.1, a confirmation that the final heights of the emplacement scale with the initial aspect ratio and are independent of the inter-granular friction is presented. Then we show results that confirm, as concluded in ([13, 16, 15]), that the emplacement properties are nearly independent of gravity. We show that, at the grain scale, there is an effect of gravity that contributes to the flow properties. Finally, in section 5 we discuss the implications of these numerical observations on the emplacement of granular materials in extraterrestrial gravities.

2. Numerical model and simulation parameters

To study the effect of varying gravity on the collapse of granular columns, numerical simulations using an Open Source Software ([4]) have been performed. This package, based on the Discrete Element Method (DEM), integrates Newton's equations of motion for each grain on the system which interact only at contact under prescribed elastic and viscous forces in the normal and tangential directions. The friction between grains is implemented using a Coulomb type model determined by the value of the inter-granular friction coefficient μ. The details of the numerical algorithm can be found in ([4]).

Columns are constructed by randomly pouring $N_t = 5000$ spherical grains constrained to move only on a 2D space between two walls whose half separation determines the initial width x_0 of the column. The simulation parameters used correspond to grains of diameter $d = 0.9mm$ with a density of $\rho =$

3

Table 1: Parameter values used for the simulations. The inter-granular friction coefficient μ and the value of gravity are changed for each column of initial aspect ration a, defined in the main tex. ($g_0 = 9.81 m/s^2$).

μ:	0.5	0.55	0.6	0.65	0.7	0.75	0.8	0.85	0.9	0.95
a:	22.53	14.63	5.75	4.55	3.70	3.08	2.58	2.20	1.67	1.50
g/g_0:	0.1	0.2	0.3	0.4	0.5	1.0	10.0			

$2500 kg/m^3$, corresponding to laboratory glass beads. Once the grains have settled and reached an equilibrium state, the maximum height of the particles, h_0, is measured and the value of the corresponding initial aspect ratio of the column is obtained as $a = h_0/x_0$. In this way 11 columns with $1.5 \leq a \leq 22.5$ are obtained. At $t = 0$ the walls are removed instantaneously, releasing the grains and initiating the collapse. Each collapse is performed starting from the same initial state and varying the inter-granular friction coefficient value from $\mu = 0.5$ to $\mu = 0.95$. For each column and each value of friction, the value of the gravitational acceleration is also changed. We considered fractional multiples of the value of gravity on Earth $g_0 = 9.81 m/s^2$. Table 1 summarizes the parameters used for the simulations.

The numerical simulations reproduce qualitatively well the deposits formed by columns collapsing under Earth's gravity, as can be seen on Fig. 8, which shows snapshots of a typical collapse at different instants for a particular column aspect ratio ($a \approx 4.5$) and an inter-granular friction value ($\mu = 0.5$) for three different values of gravitational accelerations.

In the next section we discuss the measurements performed during the collapse process to obtain information about the emplacement and the flow as gravity is varied. It will be shown that gravity can be scaled out of the list of variables, as in ([13, 16, 15]), so that the emplacements are gravity independent. Nevertheless, as it will be shown in a following section, for some specific cases gravity still has an effect in the flow.

3. Dimensional issues

If no other forces are present, dimensional analysis shows that the height h of a single grain dropped from an initial height, h_0, with an initial velocity v_0, in

a constant gravitational field g_0, can be written as

$$\frac{h}{h_0} = \Psi\left(\frac{t}{\sqrt{2h_0/g}}, \frac{v_0}{\sqrt{2gh_0}}\right), \qquad (1)$$

where Ψ is a dimensionless function. If the initial velocity is zero, the normalized height reduces to a function of a single dimensionless variable

$$\Pi = \Psi_1(\tau), \qquad (2)$$

where $\Pi \equiv \frac{h}{h_0}$ and $\tau = t(2h_0/g)^{-1/2}$ are the dimensionless height and time. The functional form of $\Psi_1(\tau)$ can, in fact, be derived analytically, and is given by $\Psi_1(\tau) = 1 - \tau^2$, which is independent of the value of gravity. This means that the height of a grain falling near the surface of Earth (where $g = 9.81m/s^2 = g_0$) or near the surface of Mars (where $g \approx 0.4g_0$) will follow the same dimensionless law given by $\Psi_1(\tau)$, provided that no other interactions exist. Considering this rather trivial observation, it is natural to ask if the collapse of a column made of many such grains will have a similar law when collapsing under different gravitational accelerations. In ([15]) a minimal model based on a shallow water approximation together with a Coulomb type friction law is proposed to describe the emplacements of columns under the action of gravitational accelerations. Scaling arguments show that the solutions of this model do not depend on gravity and that the experimentally observed scaling for low initial aspect ratios is contained in the model equations ([15]). Considering this model ([13, 16]) tried to reconcile the observations for the Valles Marineris landslides on Mars with interesting results. The dimensional arguments described above lead to the conclusion that the emplacements of granular columns do not depend on the value of gravity. However, a granular column is a complex system depending on many parameters, so a complete dimensional analysis is not feasible. The numerical simulations of the collapse of two dimensional granular columns in different gravities reported here are aimed to provide some answers to this matter. Before presenting the results, in the remaining of this section, we discuss the measurements to obtain information about the emplacement and the flow.

3.1. The maximum height function

The deposit formed when a granular column collapses depends, among other variables, on the initial geometry of the column ([8, 12, 9, 11, 6, 1]). Experimentally, the final values of the horizontal and vertical distances traveled by the grains are measured and found to scale with the initial aspect ratio $a = h_0/x_0$. In

5

this investigation we focus only on the final height. The final height h_f, or top of the column, is obtained by measuring the top of the deposit once the grains have come to rest. One of the advantages of numerical simulations is that they provide access to all the information of the system during the whole process; thus, the time evolution of the top of the deposit during the collapse is measured. We call this the maximum height function, $h_m = h_m(t)$. The measurements generally reported by the experiments are the asymptotic value of h_m:

$$h_f = \lim_{t \to \infty} h_m(t).$$

Because the final height depends on the initial geometry of the column (by means of the parameter a), considering dimensional analysis we can write

$$h^* = \Phi(\tau, a, \mu) \tag{3}$$

where

$$h^* = \frac{h_m}{h_0}, \tag{4}$$

$$\tau = \frac{t}{\sqrt{2h_0/g}}, \tag{5}$$

are the dimensionless maximum height of the deposit and the dimensionless time respectively. This dimensionless maximum height function is the equivalent to the vertical position of the falling grain example (discussed at the beginning of this section) and provides information of the collapse process under the gravitational acceleration by means of the dimensionless variable τ. The dimensionless function Φ is unknown except for some asymptotic values that can be inferred from experimental observations. As it is not yet clear how the properties of the grains affect the final results ([8, 12, 9, 11, 6, 1, 17, 19]), and even though the friction coefficient between grains μ cannot be obtained by dimensional considerations, as done in ([10]), we have included it as a relevant dimensionless variable on which the collapse may depend on. It is convenient to study, instead, the function

$$dh^* = 1 - h^* = \varphi(\tau, a, \mu), \tag{6}$$

which allows us to directly compare with the functional form $\Psi_1(\tau)$ of Eqn. 2. In terms of this function, asymptotic values of the maximum height of the deposit can be obtained from experimental observations and numerical results, considering a, μ or τ to be large or vanishingly small. We will discuss this shortly. Before that, a quantity used to characterize the flow and final state of the deposit is presented.

6

3.2. The inertial number

Recently, significant advances have been reached in the rheological description of granular flow ([2]). A single dimensionless number called the inertial number I, has been used to describe flow properties, in particular for the transient flow in the column collapse problem ([5, 7]). A quantity equivalent to the inertial number can be constructed as the ratio of two characteristic time scales of the flow during the column collapse ([18]). When the deposit experiences horizontal deformation the rate of deformation can be approximated by

$$\dot{\gamma} \approx \frac{x(t) - x_0}{t} \frac{1}{h_0 - h(t)}.$$

A characteristic time can be constructed from the pressure of the whole column at the base $P = \frac{Mg}{x - x_0}$, where M is the total mass of the column. A pressure time scale can be then constructed as

$$T_P = \hat{d} \frac{(x - x_0)^{1/2}}{\sqrt{c_0 A g}},$$

where $\hat{d}$ is the mean grain diameter and $c_0 A$ is the initial area occupied by the grains in the column. Comparing the pressure time scale with the inverse of the effective shear rate, the inertial number can be written as:

$$I = \frac{(x - x_0)^{3/2}}{h - h_0} \frac{\hat{d}}{t \sqrt{c_0 A g}}. \tag{7}$$

Large values of I indicate that the pressure of the material above dominates over horizontal deformations of the deposit ([2]), hence the flow is dense and dominated by friction between grains. We expect to observe a decrease on the value of I as time advances and the shear deformation becomes important. More important is the fact that an effective friction coefficient can be calculated, solely, as a function of I ([2]). Therefore, knowing the value of I can help to asses the amount of dissipation occurring in the flow. In the next section we show results of this quantity for the collapses of granular columns.

4. Results

In this section we present results of the numerical simulations of collapses of granular columns in different gravities. For each column with initial aspect ratio a we vary the inter-granular friction coefficient μ according to the list of values

shown in Table 1 and let the grains collapse. We then repeat this for each gravity value shown on the same table. Results are presented starting with the reference case $g = g_0$ where we find that our results are in accordance with previously published work. Then, we present results of the collapses for other values of g.

4.1. Reference case: $g = g_0$

Figure 1 shows the evolution of the top of the column normalized by the initial height (h^*, Eqn. 4) at $g = 1.0g_0$ for the extreme values of inter-granular friction considered in this study: $\mu = 0.5$ (filled symbols) and $\mu = 0.95$ (open symbols). As can be seen from the plot, some differences due to the friction coefficient between grains are most noticeable for small values of the initial aspect ratio (top most curves on Fig. 1); however, changing the friction coefficient between grains results, in general, in small differences on the evolution of the top of the column and on the final height.

The normalized final height, h_f^*, is shown in Fig. 2 as a function of the parameter a for the same data shown in Fig. 1. Columns made of grains with the lower friction coefficient ($\mu = 0.5$, filled symbols in Fig. 2) have slightly smaller heights that those made of grains with the higher friction coefficient ($\mu = 0.95$, open symbols in Fig. 2).

As many others ([8, 12, 9, 11, 6, 1, 19, 17]) we find a scaling law for the final height of the form

$$h_f^* = \lambda a^\beta. \tag{8}$$

No significant difference is observed as values of μ change and a linear relationship for $\beta = \beta(\mu)$ and $\lambda = \lambda(\mu)$ are obtained:

$$\beta(\mu) \simeq 0.06\mu - 0.80$$
$$\lambda(\mu) \simeq 0.20\mu - 0.43.$$

Clearly, the small value of the slope for $\beta(\mu)$ is indicative of the nearly null dependence of the exponent on the inter-granular friction coefficient. This seems to support the hypothesis that the scaling exponents do not depend strongly on the friction between the grains ([16, 8, 12, 9, 11, 6, 1]). On the other hand the pre-factor coefficient λ does depend weakly on μ, also consistent with previous work ([16, 6, 1]). By taking this into account, we found that the final height of the deposit scales with the initial aspect ratio parameter a according to

$$\frac{h_\infty}{h_0} \sim a^{(-0.80 \pm 0.06)} \tag{9}$$

8

when $g = 1.0g_0$. Figure 2 shows this result as a dashed line together with the final height data.

We now turn our attention to the scaling of the top of the column as the collapse occurs. Figure 3a shows the same data from Fig. 1 but for the shifted maximum height function dh^* defined by Eqn. 6. On this plot the free fall scaling law $1 - \Psi_1(\tau) = \tau^2$ is also shown by a dashed line. It can be seen that for $\tau < 1$ the columns with intermediate and large values of a follow this law. As a decreases, the collapse no longer follows the τ^2 trend. Also, for all cases, when $\tau \gtrsim 1$ the collapse no longer follows the free fall regime.

Figure 4a shows the inertial number I from Eqn. 7 for these results ($g = 1.0g_0$). The inertial number starts at a high value as the column begins to collapse, which indicates that the flow is dominated by the pressure of the material above. This pressure depends on the gravitational acceleration. As time advances this quantity decreases reaching a minimum value which depends on the initial aspect ratio of the column. Then the inertial number slightly increases again until a final value is reached that depends on a and weakly on inter-granular friction. The final values of the inertial number lie in the range of a dense flow regime ([2]) and are a decreasing function of the initial aspect ratio a. This means that flow of columns with a high initial aspect ratio is dominated by the horizontal deformation, while for columns with a small initial aspect ratio, flow is mainly determined by the pressure of the material above the emplacement. For columns with the same aspect ratio the evolution of this quantity is similar, irrespective of the friction between grains and have similar final values; thus, we expect columns with similar values of a to flow with a similar rheology in terms of the inertial number ([2]), and have similar final properties.

4.2. Collapses for other values of g.

The results presented so far correspond to the reference case of Earth's gravity $g = 1.0g_0$. The fundamental difference of columns collapsing under different gravitation accelerations with respect to the reference case is in the vertical accelerations. As discussed in Sec. 3, the height of a single grain would follow the scaling law given by Eqn. 2 and would be invariant with respect to changes in gravity. In what follows we show results of the collapse of a column to address the question if the properties of the emplacement change when occurring under different gravitational accelerations.

Figures 3b and 3c show the evolution of dh^* (Eqn. 6) for two extreme cases: $g = 0.1g_0$ and $g = 10.0g_0$. We notice that the scaling is very similar to the reference case as expected from the dimensional analysis discussed previously. This confirms that the scaling arguments of ([15]), implying that the collapses

9

should be independent of gravity, hold true. It can be observed in both cases, that the differences on the collapse depend weakly on the inter-granular friction, but strongly on the parameter a: columns with a larger initial aspect ratio follow the free-fall scaling law closer than columns with a small initial aspect ratio, specially at greater gravitational accelerations (Fig. 3c). Some differences between lower and greater gravities are more noticeable at short times $\tau < 1$ and for small aspect ratios, as if these columns took some time to react to the collapse. Since the effect of inter-granular friction is weak and does not affect the results in an important manner, in what follows we will show only data for $\mu = 0.5$. In Fig. 5 the evolution of h^* is shown for three gravitational accelerations and three different aspect ratios. Notice that for a given value of a, the top of the column follows similar curves when the emplacement occurs on different gravities. It is interesting to note that the top of columns collapsing at small gravity acceleration ($g = 0.1g_0$ continuous curves in Fig. 5) end slightly above the others, more noticeable for the largest aspect ratio (squares on Fig. 5).

In Fig. 6 we show the normalized final height h^*_f as a function of the gravity acceleration for different initial aspect ratios. It can be seen that the value of h^*_f remains fairly constant when the collapses occur on different gravitational accelerations, indicating that somehow the emplacements end with similar properties.

We now turn our attention to the inertial number as defined by Eqn. 7. Figure 4b shows the inertial number for the same data of Fig. 5. Unlike the top of the column, curves of the inertial number of collapsing columns under different gravities do not reach similar values for the same initial aspect ratio. A certain dependence on the gravity value can be observed, most noticeable when a column with an initially large aspect ratio collapses under a low value of gravity (square and solid curve in Fig 4b), for this case the inertial number is highest. In all other cases except for large gravities, the inertial number has a lower final value as the initial aspect ratio increases.

To further characterize the emplacements we performed an energy balance analysis. Following ([19, 18]), we plot the mean kinetic, potential and cumulative dissipation energy during the collapse, normalized by their respective initial energy, which is gravity dependent. Figures 7a, 7b and 7c show this energy balance for columns of Fig. 5 as they collapse under different gravities. For a given aspect ratio, the potential energy follows a similar trend for all the cases regardless of the gravitational acceleration. By the end of the process when the kinetic energy approaches zero, all emplacements with the same initial aspect ratio have a similar final value of potential energy. As discussed in ([18]), this in part explains why columns with the same initial aspect ratio have the final height

10

and thus the emplacements have a similar final geometry and scale as Eqn. 8. Columns with a large initial aspect ratio collapsing in low gravities take a longer time to loose their kinetic energy (circle and dotted line in Fig. 7a), while intermediate aspect ratio columns reach a zero kinetic energy state faster at when collapsing at low gravities (circle and dotted line in Fig. 7b). On the other hand, small aspect ratio columns convert their kinetic energy in a similar way regardless of the gravity under which they collapse, as can be seen from Fig. 7c. Notice that for all aspect ratios, the kinetic energy during the avalanche phase ([17, 18]) is slightly higher when the column collapses in the largest gravity (triangles in Figs. 7a,7b, and 7c), and slightly lower when gravity is smallest. In all cases, the cumulative dissipated energy curves are similar.

We now look at the state of the emplacement at the times marked on Fig. 4b. Figure 8 shows the state of columns with different aspect ratios at dimensionless time τ collapsing at different gravitational accelerations.

For a similar value of the aspect ratio, the grains collapsing at a lower gravity appear to be fluidized at the beginning of the emplacement, while for larger gravity accelerations, the granular mass is more compacted. As the collapse evolves, this initial fluidized state disappears and both emplacements have similar final characteristics (as the plots of Fig. 5 indicate). In this example the fluidized behavior for low gravities is observed clearly. Although the column collapsing on Earth's gravity also appears to be slightly fluidized, it can be seen that grains collapsing in the lower gravity environment show a greater spacing between them at the beginning of the emplacement. This effect is very similar to the one achieved on ([16]) by initially fluidizing the grains. Notice that as the emplacement occurs this initial fluidization effect disappears and the final deposits reach similar final properties, in accordance to the measurements of h_∞/h_0 shown in Fig. 5.

5. Discussion and Conclusions

We have performed numerical simulations of the collapses of granular columns varying the gravitational acceleration and found that the scaling

$$h_\infty/h_0 \sim a^\beta$$

is preserved. We have also provided further evidence that the scaling exponent does not depend on the inter-granular friction. When the evolution of the dimensionless height for similar initial aspect ratio columns is plotted as a function of the gravity dependent characteristic time $\tau = \sqrt{2h_0/g}$ the curves are very close to each other, irrespective of the friction between grains and the value of

11

g. This argument has been discussed by ([14]) but considering a shallow water approximation and a Coulomb-friction type model. Our discrete element simulations confirm these results. We have also found that the inertial number for all cases lies in the dense flow regime, with high(low) aspect ratio columns having smaller(larger) final values of this quantity. We found that for a given gravity, the inertial number is a decreasing function of the initial aspect ratio.

The evolution of the inertial number, I, is important because according to the recently proposed μ−rheology ([2]), the value of the effective friction coefficient can be calculated if I is known. Such a friction coefficient gives a measure of the dissipation, and therefore could be used to predict the final properties of the deposit. When the inertial number is compared for columns with similar aspect ratio collapsing at different gravities, we observe that they evolve in a similar way depending on a, transitioning from higher to lower values depending on the initial aspect ratio, and weakly on the gravitational acceleration, with high aspect ratio columns having a greater inertial number when gravity is very small.

The energy analysis shows that high aspect ratio columns loose their available kinetic energy much slower when collapsing at low gravities (Fig. 7a). For intermediate aspect ratios we observe that the kinetic energy takes longer to dissipate in small gravities (Fig. 7b), and for low aspect ratio columns the conversion of kinetic energy is similar in all gravities (Fig. 7c). In all cases the potential and the cumulative dissipated energies follows similar curves and reaches similar final values thus the final properties of the columns are similar, which, as discussed in ([18]), in part explains why the final properties of the emplacements are similar, leading to the observed scaling laws.

It could be argued that the observed differences on the conversion of kinetic energy between high and low aspect ratio columns collapsing at low gravity values are due to different mechanism occurring at the grain level that are responsible for dissipating energy in such a way that the final emplacements present similar characteristics. The advantage of numerical methods like the one used on this work allow us to explore the evolution of the system at the grain level, and when doing this, we have noticed that as the value of gravity is lower, the grains appear to be on a fluidized state during the beginning of the collapse, similar to the effect obtained in ([16]). Since vertical accelerations due to gravity are very low, the grains that collapse at low gravities show less contacts and appear fluidized in a natural way, thus dissipating fewer energy by frictional contacts, which explains the slow conversion of kinetic energy observed in Fig. 7a for high aspect ratio columns in low gravity values. On the other extreme, grains of columns collapsing at large gravities have greater vertical accelerations and

tend to compact and present enduring contacts, dissipating energy much faster. It appears that a fine balance exists between the accelerations due to gravity and the energy dissipated by frictional contacts that makes the system's final state posses similar characteristics, irrespective of the gravitational accelerations. The inertial number I could provide some further understanding of the responsible mechanism for energy dissipation. Based on the ideas of the $\mu-$rheology, the effective friction of a granular flow depends on the inertial number solely, so flows with similar inertial numbers should present a similar effective friction. We have shown that columns collapsing at low gravities present larger values of this inertial number, thus fewer contacts between grains occur during the flow, a conclusion that can be corroborated by the fluidized effect described above, and so the dissipated energy by friction is reduced but according to the $\mu-$rheology, the effective friction increases with increasing I ([2, 3]) so that according to our measurements, a column collapsing at a low gravity has a large effective friction thus balancing the lack of dissipation by frictional contacts and ending in similar deposits as columns collapsing at higher gravities, where the value of the inertial number is lower and energy is dissipated by enduring friction contacts.

We conclude that although gravity can be scaled out of the parameters that affect the collapse, there is still an effect due to the granular nature of the system that consists on a naturally occurring fluidization effect similar to that explored experimentally in ([16]). This effect, which cannot be captured by simple continuous models, could contribute to the low effective friction and large run-out distances observed on extraterrestrial events like those of the Valles Marineris landslides on Mars.

[1] Balmforth, N. J., Kerswell, R. R., 2005. Granular collapse in two dimensions. Journal of Fluid Mechanics 538, 399–428.
URL http://www.journals.cambridge.org/abstract_S0022112005005537

[2] GDR MiDi, 2004. On dense granular flows. European Physical Journal E 14, 341–365.
URL http://www.springerlink.com/index/a94jmg12r9dyw45e.pdf

[3] Jop, P., Forterre, Y., Pouliquen, O., Jun. 2006. A constitutive law for dense granular flows. Nature 441 (7094), 727–30.
URL http://www.ncbi.nlm.nih.gov/pubmed/16760972

[4] Kloss, C., Goniva, C., 2010. LIGGGHTS:A new open sorce Discrete Element simulation software. In: Proc. of The Fifth International Conference on Discrete Element Methods.

[5] Lacaze, L., Kerswell, R. R., Mar. 2009. Axisymmetric granular collapse: a transient 3D flow test of viscoplasticity. Physical Review Letters 102 (10), 108305.
URL http://www.ncbi.nlm.nih.gov/pubmed/19392169

[6] Lacaze, L., Phillips, J. C., Kerswell, R. R., 2008. Planar collapse of a granular column: Experiments and discrete element simulations. Physics of Fluids 20 (6), 063302.
URL http://link.aip.org/link/PHFLE6/v20/i6/p063302/s1&Agg=doi

[7] Lagrée, P.-Y., Staron, L., Popinet, S., Sep. 2011. The granular column collapse as a continuum: validity of a two-dimensional NavierStokes model with a μ(I)-rheology. Journal of

Fluid Mechanics 686, 378–408.
URL http://www.journals.cambridge.org/abstract_S0022112011003351

[8] Lajeunesse, E., Mangeney-Castelnau, A., Vilotte, J. P., 2004. Spreading of a granular mass on a horizontal plane. Physics of Fluids 16, 2371–2381.
URL http://pof.aip.org/resource/1/phfle6/v16/i7/p2371_s1

[9] Lajeunesse, E., Monnier, J. B., Homsy, G. M., 2005. Granular slumping on a horizontal surface. Physics of Fluids 17 (10), 103302.
URL http://link.aip.org/link/PHFLE6/v17/i10/p103302/s1&Agg=doi

[10] Lajeunesse, E., Quantin, C., Allemand, P., Delacourt, C., 2006. New insights on the runout of large landslides in the Valles-Marineris canyons, Mars. Geophysical Research Letters 33 (4), 2–5.
URL http://www.agu.org/pubs/crossref/2006/2005GL025168.shtml

[11] Lube, G., Huppert, H. E., Sparks, R. S. J., Freundt, A., 2005. Collapses of two-dimensional granular columns. Physical Review E 72, 041301.
URL http://pre.aps.org/abstract/PRE/v72/i4/e041301

[12] Lube, G., Huppert, H. E., Sparks, R. S. J., Hallworth, M. A., Jun. 2004. Axisymmetric collapses of granular columns. Journal of Fluid Mechanics 508, 175–199.
URL http://www.journals.cambridge.org/abstract_S0022112004009036

[13] Lucas, A., Mangeney, A., May 2007. Mobility and topographic effects for large Valles Marineris landslides on Mars. Geophysical Research Letters 34 (10), 1–5.
URL http://www.agu.org/pubs/crossref/2007/2007GL029835.shtml

[14] Mangeney, A., Heinrich, P., Roche, R., Aug. 2000. Analytical Solution for Testing Debris Avalanche Numerical Models. Pure and Applied Geophysics 157 (6-8), 1081–1096.
URL http://www.springerlink.com/openurl.asp?genre=article&id=doi:10.1007/s000240050018

[15] Mangeney-Castelnau, A., Bouchut, F., Vilotte, J. P., Lajeunesse, E., Aubertin, A., Pirulli, M., 2005. On the use of Saint Venant equations to simulate the spreading of a granular mass. Journal of Geophysical Research 110 (B9), 1–17.
URL http://www.agu.org/pubs/crossref/2005/2004JB003161.shtml

[16] Roche, O., Attali, M., Mangeney, A., Lucas, A., Nov. 2011. On the run-out distance of geophysical gravitational flows: Insight from fluidized granular collapse experiments. Earth and Planetary Science Letters 311 (3-4), 375–385.
URL http://linkinghub.elsevier.com/retrieve/pii/S0012821X11005371

[17] Staron, L., Hinch, E. J., Dec. 2005. Study of the collapse of granular columns using two-dimensional discrete-grain simulation. Journal of Fluid Mechanics 545 (-1), 1.
URL http://www.journals.cambridge.org/abstract_S0022112005006415

[18] Tapia-McClung, H., Zenit, R., 2012. Computer simulations of the collapse of columns formed by elongated grains. Physical Review E 85 (6), 061304.
URL http://link.aps.org/doi/10.1103/PhysRevE.85.061304

[19] Zenit, R., 2005. Computer simulations of the collapse of a granular column. Physics of Fluids 17, 031703.
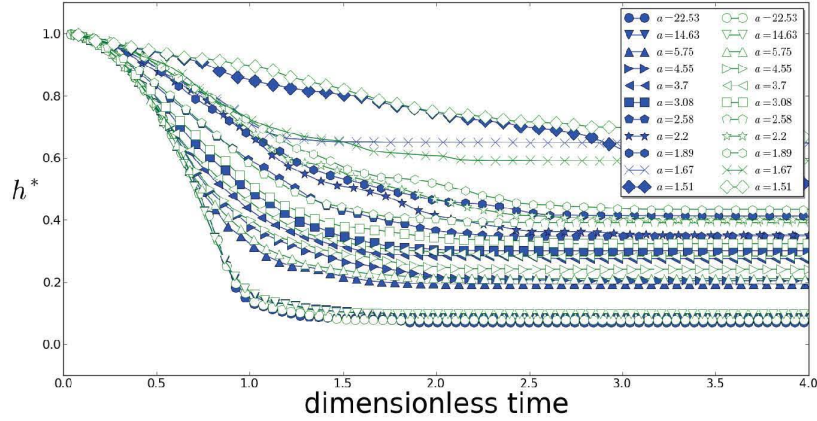URL http://link.aip.org/link/?PHFLE6/17/031703/1

Figure 1: (Color online) Evolution of the top of the column for the different values of the parameter a and for the two extreme values of inter-granular friction explored (see Table 1). Filled blue symbols show data for $\mu = 0.5$ and open green symbols for $\mu = 0.95$. Different symbols correspond to values of the parameter a as shown in the box.
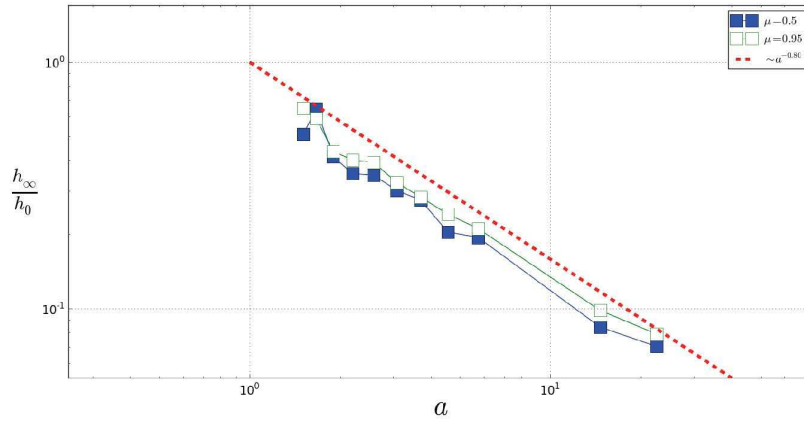

Figure 2: (Color online). Normalized final height h_f^* as a function of the initial aspect ratio for the data of Fig. 1. Blue open symbols show data for $\mu = 0.5$, while green dark symbols show data for $\mu = 0.95$. The red dashed line is the best fit corresponding to the scaling law Eqn. 9.

(a) $g = 1.0g_0$

(b) $g = 0.1g_0$

(c) $g = 10.0g_0$
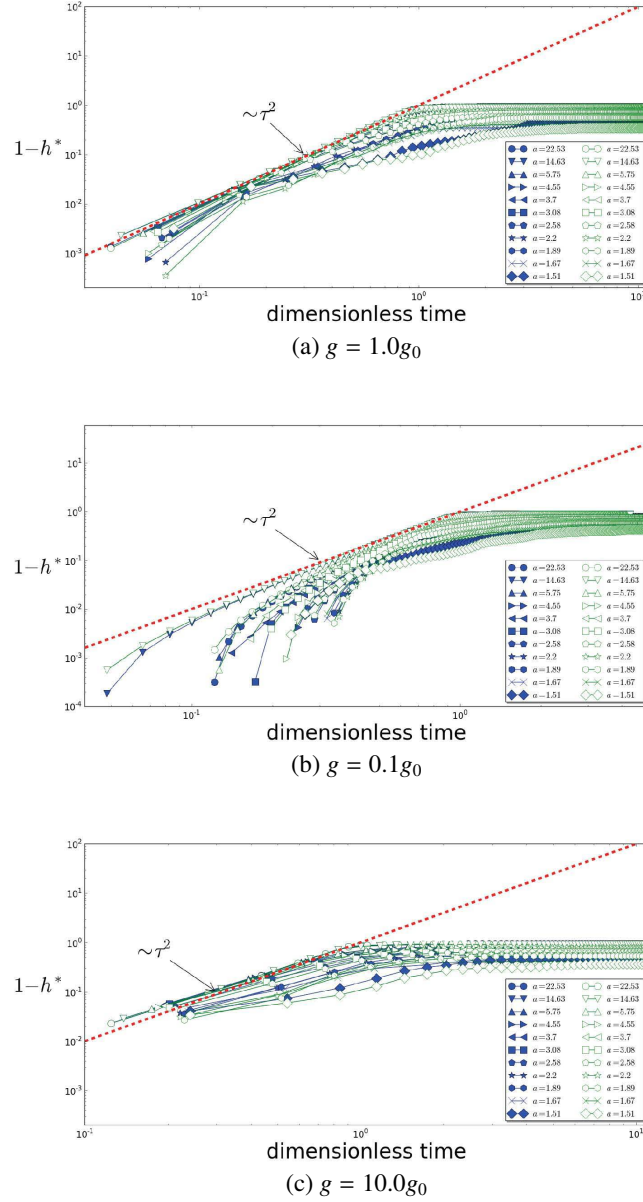
Figure 3: (Color online) Evolution of the shifted maximum function (dh^*, Eqn. 6) for columns with different values of the parameter a and inter-granular friction μ with gravity acceleration $g = 1.0g_0, 0.1g_0$ and $10.0g_0$. Symbols are the same as in Fig. 2, with open blue symbols showing data for $\mu = 0.5$ and green filled symbols for $\mu = 0.95$. The dashed red line shows the free fall scaling law $\sim \tau^2$ and the arrow indicates the direction of decreasing a values.
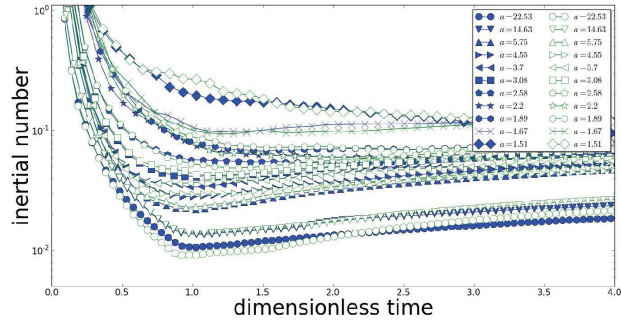
(a) $g = 1.0g_0$
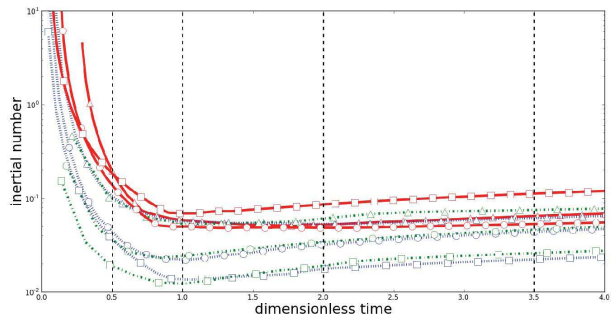
(b) $g = 0.1g_0$

Figure 4: Inertial number (I, Eqn.7) for the same data parameters of Fig. 3a (4a) and Fig. 6 (4b). Dashed red vertical lines on Fig. 4b correspond to the dimensionless times at which the snapshots of Fig. 8 where taken.
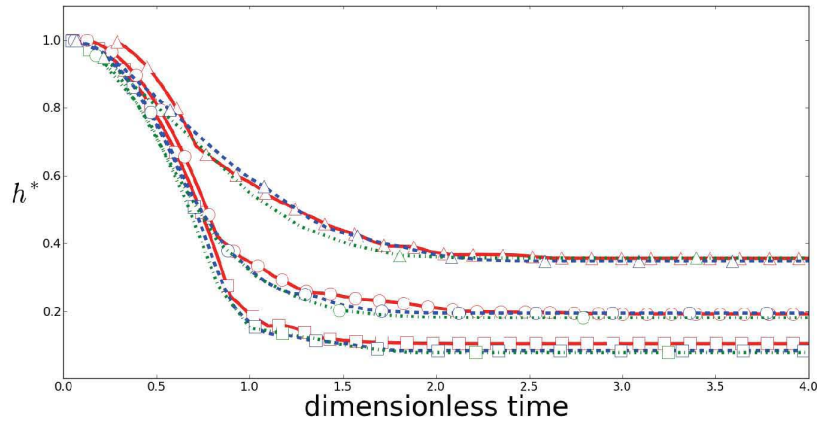
Figure 5: Evolution of h^* for columns collapsing under different gravity accelerations: red curves $g = 0.1g_0$, blue curves $g = g_0$ and green curves $g = 10g_0$, and for different initial aspect ratios: squares $a = 14.62$, circles $a = 5.75$ and triangles $a = 2.58$. The inter-granular friction value is fixed at $\mu = 0.5$ in all cases show.
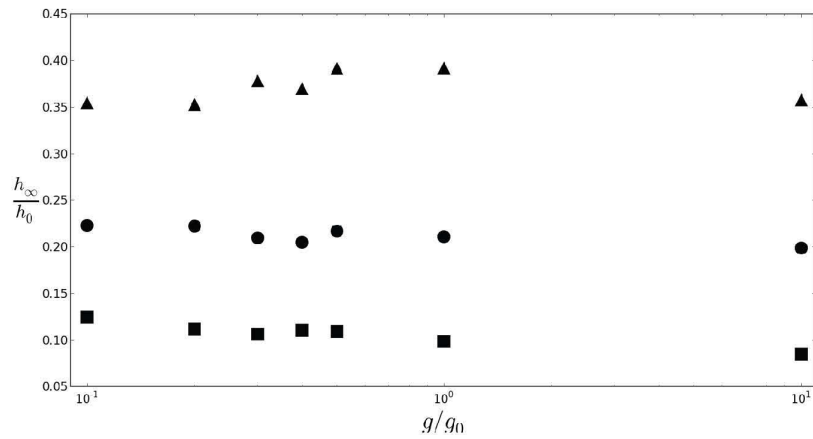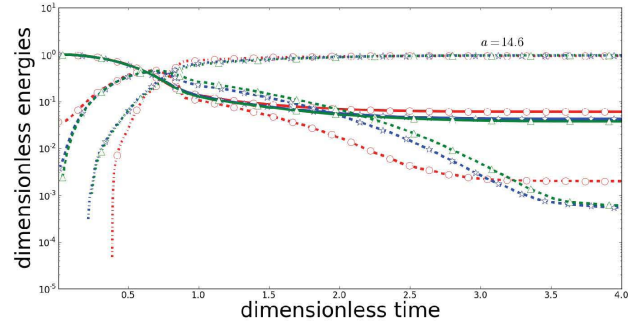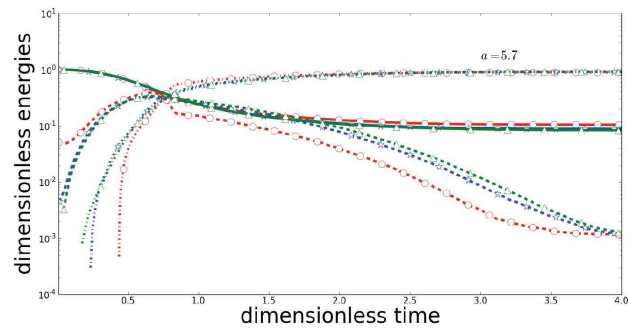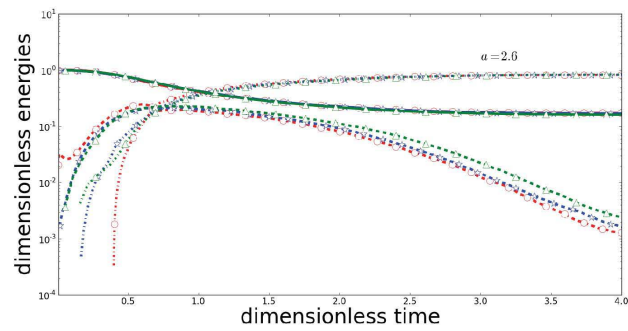

Figure 6: Normalized final height h_f^* as a function of g/g_0. Squares correspond to the initial aspect ratio $a = 14.6$, circles $a = 5.7$ and triangles $a = 2.6$.

(a) $a = 14.6$

(b) $a = 5.7$

(c) $a = 2.6$

Figure 7: (Color online) Energy balance for columns of initial aspect ratio $a = 14.6, 5.7, 2.6$. Solid lines indicate potential energy; dotted lines represent kinetic energy and dash-dot lines the energy difference $E_d = 1 - E_p - E_k$. Red circle symbols correspond to $g = 0.1g_0$; blue stars $g = g_0$ and green triangles $g = 10g_0$.

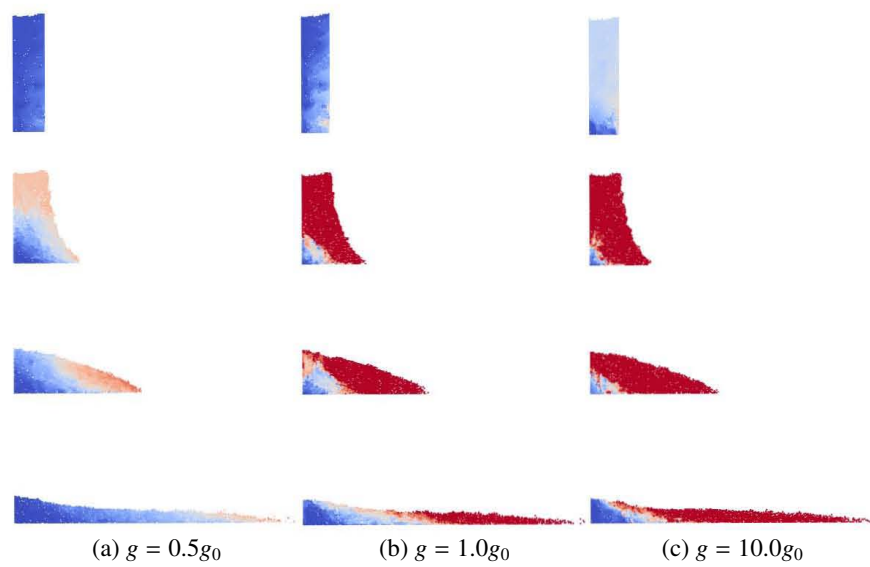(a) $g = 0.5g_0$ (b) $g = 1.0g_0$ (c) $g = 10.0g_0$

Figure 8: Emplacement comparison in three different gravitational accelerations $g/g_0 = 0.5, 1.0, 10.0$ for the same initial low aspect ratio $a \simeq 4.5$ at dimensionless times marked on Fig. 4b, $\tau \approx 0.0, 0.5, 1.0, 2.0$ (from top to bottom). Each column shows the collapse under a gravity with value $g/g_0 = 0.5, 1.0, 10.0$. Blue (slow) to red (fast) colors indicate increasing grain speed. Note that only the right side of the collapses are shown as they are very symmetric.

REFERENCES

[1] M. P. Allen and D. J. Tildesley, *Computer Simulation of Liquids*, Oxford University Press, USA, 1989.

[2] H. C. Andersen, *Rattle: A velocity version of the shake algorithm for molecular dynamics calculations*, Journal of Computational Physics **52** (1983), no. 1, 24–34.

[3] N. J. Balmforth and R. R. Kerswell, *Granular collapse in two dimensions*, Journal of Fluid Mechanics **538** (2005), 399–428.

[4] G. I. Barenblatt, *Scaling, Self-similarity, and Intermediate Asymptotics: Dimensional Analysis and Intermediate Asymptotics (Cambridge Texts in Applied Mathematics)*, Cambridge University Press, 1996.

[5] ———, *Scaling*, Cambridge University Press, 2003.

[6] D.l Blair, T. Neicu, and A. Kudrolli, *Vortices in vibrated granular rods*, Physical Review E **67** (2003), no. 3.

[7] P. W. Bridgman, *Dimensional Analysis*, Yale University Press, 1922.

[8] V. Chugunov, J.M.N.T. Gray, and K. Hutter, *Some Invariant Solutions of the Savage Hutter Model*, Proceedings of Institute of Mathematics of NAS of Ukraine **43** (2002), no. 5, 111–119.

[9] A. Daerr and S. Douady, *Sensitivity of granular surface flows to preparation*, Europhysics Letters **47** (1999), 324.

[10] L. J. Daniels, Y. Park, T. C. Lubensky, and D. J. Durian, *Dynamics of Gas-Fluidized Granular Rods*, Physical Review E **79** (2008), no. 4 Pt 1, 041301.

[11] E. E. Doyle, H. E. Huppert, G. Lube, H. M. Mader, and R. S. J. Sparks, *Static and flowing regions in granular collapses down channels: Insights from a sedimenting shallow water model*, Physics of Fluids **19** (2007), no. 10, 106601.

[12] Scott V. Franklin, *Geometric cohesion in granular materials*, Physics Today **65** (2012), no. 9, 70 (en).

[13] GDR MiDi, *On dense granular flows*, European Physical Journal E **14** (2004), 341–365.

[14] J. Gratton and C. Vigo, *Self-similar gravity currents with variable inflow revisited : plane currents*, Journal of Fluid Mechanics **258** (1994), 77–104.

[15] Nick Gravish, Scott Franklin, David Hu, and Daniel Goldman, *Entangled Granular Media*, Physical Review Letters **108** (2012), no. 20, 208001.

[16] H. Jaeger, S. Nagel, and R. Behringer, *Granular solids, liquids, and gases*, Reviews of Modern Physics **68** (1996), no. 4, 1259–1273.

[17] P. Jop, Y. Forterre, and O. Pouliquen, *A constitutive law for dense granular flows.*, Nature **441** (2006), no. 7094, 727–30.

[18] L. Kadanoff, *Built upon sand: Theoretical ideas inspired by granular flows*, Reviews of Modern Physics **71** (1999), no. 1, 435–444.

[19] R. R. Kerswell, *Dam break with Coulomb friction: A model for granular slumping?*, Physics of Fluids **17** (2005), no. 5, 057101.

[20] C. Kloss and C. Goniva, *LIGGGHTS A new open source discrete element simulation software*, Proc. of The Fifth International Conference on Discrete Element Methods, 2010.

[21] L. Lacaze and R. R. Kerswell, *Axisymmetric granular collapse: a transient 3D flow test of viscoplasticity.*, Physical Review Letters **102** (2009), no. 10, 108305.

[22] L. Lacaze, J. C. Phillips, and R. R. Kerswell, *Planar collapse of a granular column: Experiments and discrete element simulations*, Physics of Fluids **20** (2008), no. 6, 063302.

[23] P.Y. Lagrée, L. Staron, and S. Popinet, *The granular column collapse as a continuum: validity of a two-dimensional Navier–Stokes model with a μ(I)-rheology*, Journal of Fluid Mechanics **686** (2011), 378–408.

[24] E. Lajeunesse, A. Mangeney-Castelnau, and J. P. Vilotte, *Spreading of a granular mass on a horizontal plane*, Physics of Fluids **16** (2004), 2371–2381.

[25] E. Lajeunesse, J. B. Monnier, and G. M. Homsy, *Granular slumping on a horizontal surface*, Physics of Fluids **17** (2005), no. 10, 103302.

[26] E. Lajeunesse, C. Quantin, P. Allemand, and C. Delacourt, *New insights on the runout of large landslides in the Valles-Marineris canyons, Mars*, Geophysical Research Letters **33** (2006), no. 4, 2–5.

[27] E. Larrieu, L. Staron, and E. J. Hinch, *Raining into shallow water as a description of the collapse of a column of grains*, Journal of Fluid Mechanics **554** (2006), 259–270.

[28] G. Lube, H. E. Huppert, R. S. J. Sparks, and A. Freundt, *Collapses of two-dimensional granular columns*, Physical Review E **72** (2005), 041301.

[29] _____ , *Static and flowing regions in granular collapses down channels*, Physics of Fluids **19** (2007), no. 4, 043301.

[30] G. Lube, H. E. Huppert, R. S. J. Sparks, and M. A. Hallworth, *Axisymmetric collapses of granular columns*, Journal of Fluid Mechanics **508** (2004), 175–199.

[31] A. Lucas and A. Mangeney, *Mobility and topographic effects for large Valles Marineris landslides on Mars*, Geophysical Research Letters **34** (2007), no. 10, 1–5.

[32] A. Mangeney, P. Heinrich, and R. Roche, *Analytical Solution for Testing Debris Avalanche Numerical Models*, Pure and Applied Geophysics **157** (2000), no. 6-8, 1081–1096.

[33] A. Mangeney-Castelnau, F. Bouchut, J. P. Vilotte, E. Lajeunesse, A. Aubertin, and M. Pirulli, *On the use of Saint Venant equations to simulate the spreading of a granular mass*, Journal of Geophysical Research **110** (2005), no. B9, 1–17.

[34] T. Pöschel and T. Schwager, *Computational granular dynamics*, Classical Continuum Physics, Springer, 2004.

[35] D. C. Rapaport, *The Art of Molecular Dynamics Simulation*, Cambridge University Press, 2004.

[36] O. Roche, M. Attali, A. Mangeney, and A. Lucas, *On the run-out distance of geophysical gravitational flows: Insight from fluidized granular collapse experiments*, Earth and Planetary Science Letters **311** (2011), no. 3-4, 375–385.

[37] D. Sahin, N. Antar, and T. Ozer, *Lie group analysis of gravity currents*, Nonlinear Analysis: Real World Applications **11** (2010), no. 2, 978–994.

[38] A. A. Sonin, *The Physical Basis of Dimensional Analysis*, 2nd ed., MIT, Cambridge, MA 02139, 2001.

[39] L. Staron and E. J. Hinch, *Study of the collapse of granular columns using two-dimensional discrete-grain simulation*, Journal of Fluid Mechanics **545** (2005), no.-1, 1.

[40] ———, *The spreading of a granular mass: role of grain properties and initial conditions*, Granular Matter **9** (2006), no. 3-4, 205–217.

[41] H. Tapia-McClung and N. Gr-Jensen, *Non-iterative and exact method for constraining particles in a linear geometry*, Journal of Polymer Science Part B: Polymer Physics **43** (2005), no. 8, 911–916.

[42] H. Tapia-McClung and R. Zenit, *Computer simulations of the collapse of columns formed by elongated grains*, Physical Review E **85** (2012), no. 6, 061304.

[43] E. L. Thompson and H. E. Huppert, *Granular column collapses: further experimental results*, Journal of Fluid Mechanics **575** (2007), 177.

[44] M. Trepanier and S. Franklin, *Column collapse of granular rods*, Physical Review E **82** (2010), 1–5.

[45] D. Volfson, A. Kudrolli, and L. Tsimring, *Anisotropy-driven dynamics in vibrated granular rods*, Physical Review E **70** (2004), no. 5, 051312.

[46] R. Zenit, *Computer simulations of the collapse of a granular column*, Physics of Fluids **17** (2005), 031703.